RSC Advances

This is an *Accepted Manuscript*, which has been through the Royal Society of Chemistry peer review process and has been accepted for publication.

Accepted Manuscripts are published online shortly after acceptance, before technical editing, formatting and proof reading. Using this free service, authors can make their results available to the community, in citable form, before we publish the edited article. This *Accepted Manuscript* will be replaced by the edited, formatted and paginated article as soon as this is available.

You can find more information about *Accepted Manuscripts* in the **Information for Authors**.

ROYAL SOCIETY
OF **CHEMISTRY**

www.rsc.org/advances

1   **Influence of plasma macronutrient levels on Hepatic metabolism:Role of**

2   **regulatory networksin homeostasis and disease states**

3   **Pramod R. Somvanshi[1], Anilkumar K. Patel[1], Sharad Bhartiya[2] and K.V. Venkatesh[1]**

4   *[1]Biosystems Engineering Lab, Department of Chemical Engineering,*

5   *Indian Institute of Technology Bombay, Powai, Mumbai, INDIA 400076*

6   *[2]Control systems Engineering Lab,Department of Chemical Engineering,*

7   *Indian Institute of Technology Bombay, Powai, Mumbai, INDIA 400076*

8   **Corresponding Author Email- venks@iitb.ac.in**

11

12

13

14

15

16

17

18

19 **Abstract**

20 Human liver acts as a homeostatic controller for maintaining the normal levels of plasma

21 metabolite concentrations by uptake, utilization, storage and synthesis of essential metabolites.

22 These hepatic functions are orchestrated through a multilevel regulation composed of metabolic,

23 signaling and transcriptional networks. Plasma macronutrients namely, glucose, amino acids and

24 fatty acids are known to influence these regulatory mechanisms to facilitate homeostasis. We

25 composed a regulatory circuit that elicits the design principle behind the metabolic regulation in

26 liver.We have developed a detailed dynamic model for hepatic metabolism incorporating the

27 regulatory mechanisms at signaling and transcriptional level. The model was analyzed to capture

28 the behavior of hepatic metabolic fluxes under various combinations of plasma macronutrient

29 levels. The model was used to rationalize and explain the experimental observations of metabolic

30 dysfunctions through regulatory mechanisms. We addressed the key questions such as, how high

31 carbohydrate diet increases cholesterol and why a high protein diet would reduce it; how high fat

32 and high protein diet increases gluconeogenesis leading to hyperglycemia; how

33 TCA(tricarboxylic acid)cycle is impaired through diet induced insulin resistance; how high fat

34 can impair plasma ammonia balance; how high plasma glucose can lead to dyslipidemia and

35 fatty liver disease etc. The analysis indicates that higher levels (above 2.5-3 fold) of

36 macronutrient in plasma results in impairment of metabolic functions due to perturbations in the

37 regulatory circuit. While higher glucose levels saturate the rate of plasma glucose uptake, higher

38 amino acids activate glucagon and inhibit IRS(Insulin receptor substrate)through S6K (S6

39 kinase), whereas higher fatty acid levels inhibit IRS through DAG-PKC (diacylglycerol and

40 protein kinase C)and TRB3 activation. Moreover the ATP-ADP ratio is reduced under such

41 conditions and β-oxidation is up-regulated through activation of PPARα (peroxisome

42 proliferator-activated receptor alpha)leading to reduced anabolic capacity and increased

43   cataplerosis in TCA cycle. The above factors together decrease insulin sensitivity and enhances

44   glucagon effect through underlying signaling and transcriptional network leading to insulin

45   resistance in liver. Such a metabolic state is known to result in diabetes and non-alcoholic fatty

46   liver disease.

47   **Introduction**

48   The plasma homeostasis of most of the vital metabolites is maintained by the interventions of

49   hepatic metabolism (1,2).The versatility of the central metabolic pathway in liver, enables it to

50   interconvert the metabolites and maintain hepatic energy supply when required(3,4).Due to the

51   non-linear nature of the effect of glucose, amino acids and fatty acids on insulin and glucagon

52   secretions and subsequent signaling pathway, it is difficult to predict the metabolic changes that

53   can be induced through different macronutrient compositions in diet.It is long known that dietary

54   and behavioral patterns of individuals are responsible for lifestyle diseases and the underlying

55   changes in the metabolic status(5). Several experimental investigations over the last two decades

56   have reported the effect of variation in dietary composition on hepatic metabolism in mice, rats,

57   hamsters and humans (6–14). However, such studies do not provide a mechanistic explanation

58   for the phenotypic observations such as, how a high fat and high protein diet increases

59   gluconeogenesis and hyperglycemia; How a high carbohydrate diet increases cholesterol levels;

60   How a high protein-low fat diet can reduce cholesterol synthesis; How high fat diet induce

61   defects in TCA flux leading to an insulin resistance state; How a high fat diet increases plasma

62   ammonia levels; How high plasma fat and protein levels can affect hepatic glucose release

63   leading to hyperglycemia; How high glucose levels can affect hepatic fatty acid uptake and lead

64   to dyslipidemia and NAFLD (non-alcoholic fatty lever disease) etc.

65   Our aim of this study was to develop a mechanistic model to answer these questions in a

66   regulatory perspective.To analyze these effects we developed a mathematical model

67   incorporating the regulatory circuit in the hepatic metabolism. Unlike the other models in

68   literature, this is a first effort in literature to integrate the regulatory circuit comprising of

69   signaling and transcriptional network with metabolic network. This would enable to rationalize

70   the phenotypic responses and associated disease states through a regulatory perspective.

71   The developed model was used to obtain steady state fluxes for various metabolic reactions in

72   response to variation in plasma metabolite levels. The analysis reveals that extremely high levels

73   of fatty acids and amino acids can reduce insulin sensitivity compromising the anabolic capacity

74   of insulin and consequently leading to a metabolic state that represents insulin resistance. Certain

75   combinations in the levels of macronutrients would result in metabolic fluxes that represent a

76   diabetic state wherein the hepatic glucose release, gluconeogenesis and lipolysis are active even

77   under high insulin levels (15). Conversely, under low glucose conditions (higher physical

78   activity and exercise) where a catabolic state is anticipated, with increasing circulating levels of

79   fatty acids and triglycerides reduces the catabolic capacity. Whereas, higher amino acids would

80   help in increasing the overall catabolic rate and facilitate higher rate of glucose release. Thus, the

81   study highlights the metabolic states attained due to various levels of macronutrients in plasma

82   and subsequent complexity in the regulation that leads to disease states.

83   **Regulatory Circuit**

84   Apart from being used as metabolic substrates,plasma macronutrients (glucose, amino acids and

85   lipids)act as global regulators of metabolic pathways(16,17). The regulatory actions are mediated

86   by hormones that are triggered by sensing these metabolites through pancreas. The plasma levels

87   of these macronutrients are known to influence the secretion of hormones namely, insulin and

88   glucagon (18–20). The hormones (insulin and glucagon) further activate specific signaling

89   pathways that eventually influence the activity of the downstream enzymes that catalyze

90   metabolism. These macronutrients also regulate the signaling components and transcriptional

91   factors that regulate gene expression mediated by insulin and glucagon in a highly nonlinear

92   manner (21–23). These effects of macronutrients on hormonal secretion, signaling pathways and

93   transcriptional factors result in a metabolic regulatory pattern that varies with different levels of

94   macronutrients present in the plasma. The interactions and crosstalk between the signaling,

95   transcription and metabolic pathways (as reported in several bits and parts in literature) were

96   used to develop a comprehensive regulatory circuit. While glucose enhances insulin secretion

97   and reduces glucagon secretion, amino acids have a tendency to enhance the secretion of both

98   insulin and glucagon at different thresholds (24–26). Fatty acids and triglycerides also influence

99   insulin secretion (27). Although fatty acids increase insulin secretion, it inhibits insulin signaling

100   beyond a certain threshold (28,29). The regulatory mechanisms of these macronutrients at

101   multiple levels results in a highly non-linear metabolic flux landscape based upon the different

102   quantities of these macronutrients in the diet. This leads to a complex interplay of metabolites,

103   signaling proteins and gene expression that decides the cellular metabolic state.The schematic of

104   the interactions between macronutrients, hormones and signaling is shown in Figure (1). The

105   detailed molecular network of the regulatory pathways is depicted in S1 Fig.1*.
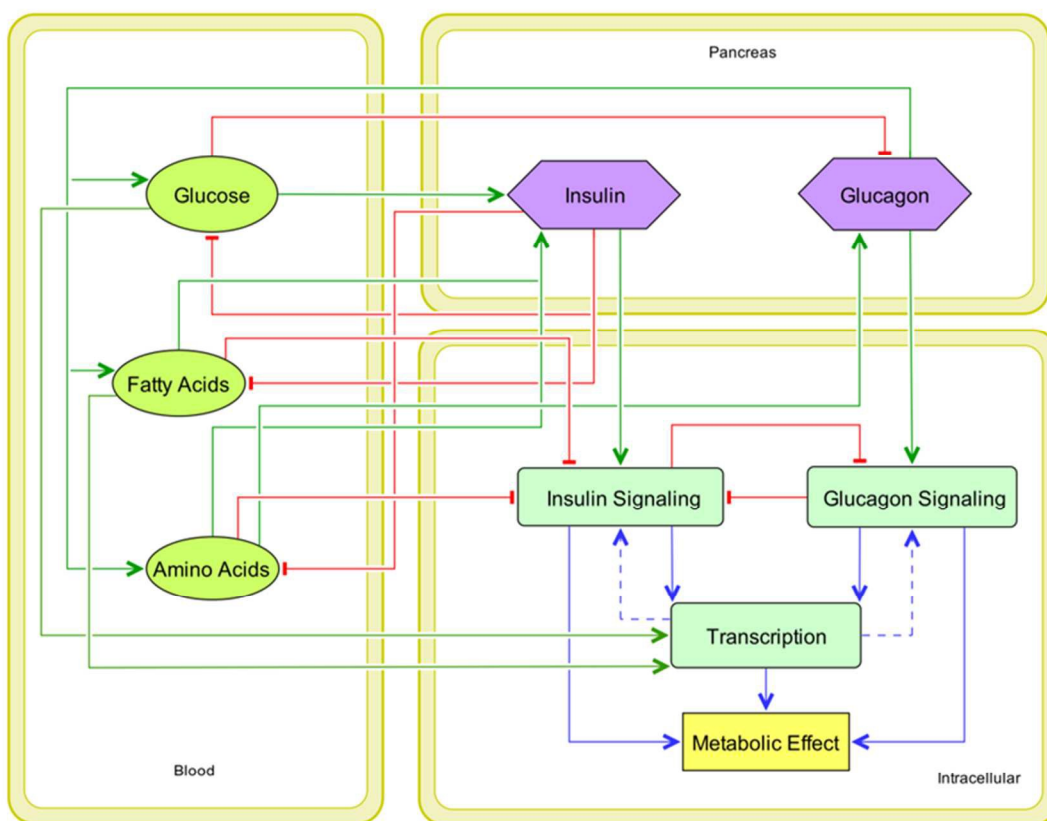
106

107 **Figure 1**   The Schematic of the interactions between plasma macronutrients (glucose, amino

108 acids and fatty acids) on pancreatic hormones (insulin and glucagon) and metabolic regulatory

109 signaling pathways.

110 **Results**

111 **Model Development**

112 In order to provide an explanation to the experimental observations, a detailed model was

113 developed incorporating hepatic metabolism (see Fig.2) and its regulation through hormonal

114 signaling and transcriptional network as shown in figure 1.In our study, we mainly concentrate

115 on the effects of plasma glucose, amino acids and fatty acid concentration on the hepatic

116 metabolism and explain several observed phenotypic responses to different dietary conditions

117 from a regulatory perspective. Moreover, this is the first time in literature, that we have

118   integrated the signaling and transcriptional effects with metabolism and have analyzed the effect

119   of plasma macronutrient concentration on the tissue metabolism. However, it should be noted

120   that there are several models that specifically model signaling or the metabolic pathways

121   independently (30–41).We have integrated these several published models as components of our

122   comprehensive modelalong with a module for whole body plasma metabolite homeostasis.We

123   applied a system level approach that is composed of four modules such as blood, metabolism,

124   signaling and transcription. The modeling framework involved representation of biological

125   pathways by mathematical functions given by mass action, Michalis-Menten and Hills kinetic

126   functions. A mass balance was performed on the network to obtain the ordinary differential

127   equations to capture the dynamics of each state variable in the system. The overall model is

128   composed of 272 rate equations, 170 state variables and 801 parameters. For details on

129   development of each module and integration see methodology section. The model was developed

130   and simulated using Matlab 2014b (mathworks.com).

131
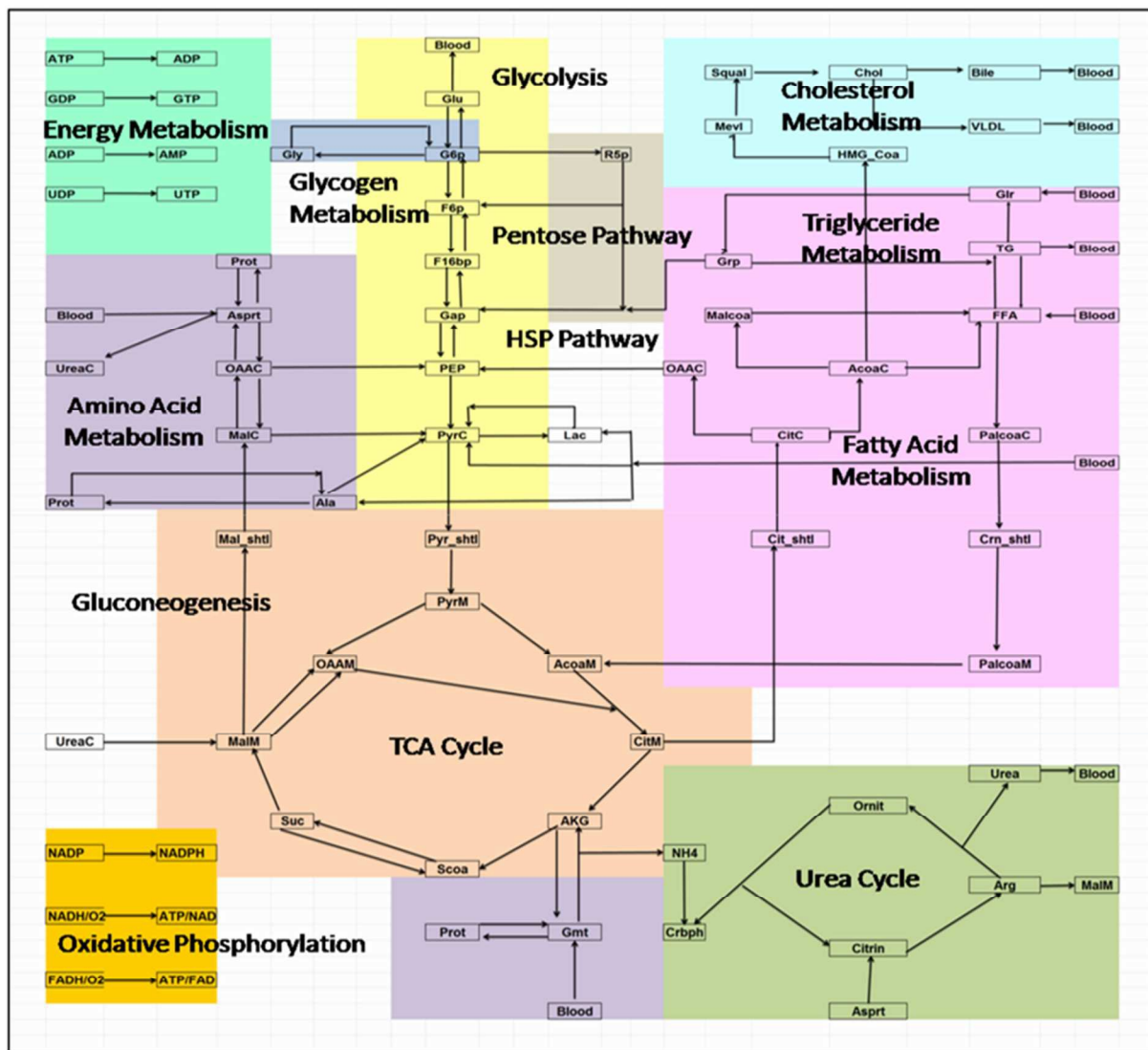
Figure 2 The Schematic of the metabolic network of the Hepatic Metabolism used in the model.

133   **Model Calibration**

134   The model was calibrated from the source/component models referred from the literature. The

135   parameters for hepatic metabolism were extracted from Konig et al. 2012 and Xu et al. 2011 (38,

136   42), for insulin signaling from Sedaghat et al 2002(43), for glucagon signaling from Xu et al.

137   2011 and Mutalik et al 2005(42, 44), for mTOR signaling from Vinod and Venkatesh 2009(45)

138   ,and Insulin secretion kinetics from Dalla Mann et al 2007(46). We tried to retain the reported

139   parameter values from the source models allowing minimal deviation in them. The parameters

140   for the model integration and optimization were estimated by the authors using optimization

141   algorithms in Matlab. We used modular partial calibration methodology wherein each subsystem

142   was optimized separately to a desired response and further integrated and re-calibrated to yield

143   the similar optimal solutions.

Model Validation

145   The model was validated by obtaining the dynamic concentration profiles of various metabolites

146   and signaling molecules for resting state during 24hr fasting condition and comparing it with the

147   literature data and the simulation results of the source models(SeeS1 file FiguresM1, M2 (I),M2

148   (II) and M2 (III)). The model was validated to capture the reported qualitative behavior of the

149   concentration profiles while the quantitative information was retained by matching the fold

150   changes or the observed rates over the time frames.For most of the concentration profiles we

151   used human data reported in literature;however we resorted to thescaled data from other animal

152   models such as mouse and rats in the instances of lacking human data.

153   The dynamic profiles indicate that the storage compounds such as glycogen and triglycerides are

154   degraded to maintain the other metabolites at a homeostatic level. The values matched the known

155   homeostatic levels reported in literature (See S1 file FiguresM2 (I) and M2 (II)). It can be noted

156   that the regulators of the storage compounds, for example, mTOR (mammalian target of

157   rapamycin) for Amino acids, GSK3 (glycogen synthase kinase 3) for glycogen and SREBP

158   (sterol response element binding protein) and PPARα and PPARβ (peroxisome proliferator-

159   activated receptoralpha and beta)for triglycerides, also show unsteady behavior causing the

160   storage compounds to be degraded. The key signaling molecules in the insulin signaling pathway

161   attain a basal steady state since the pathway is not operational under fasting conditions(See S1

162   file Fig M2 (III) A,B&C). However, during fasting, the glycogen signaling pathway is

163   operational indicated by the activation of signaling molecules cAMP (cyclic adenosine

164   monophosphate) and PKA (protein kinase A)(See S1 file Fig.M2(III) D, &E). The model for

165   transcriptional network yielded the reported qualitative trends under resting and postprandial

166   conditions (See S1 file Fig.M2(III) G, H and I).The model was thus able to compare the

167   physiological resting state thereby obtaining the steady state fluxes of various metabolic

168   reactions.

169   **Steady State Metabolic Flux Distribution**

170   The model was further used to determine/predict the effect of plasma macronutrient

171   concentration on the steady state fluxes in the various metabolic pathways. Steady sate fluxes

172   were obtained for different levels of plasma macronutrient (glucose, fatty acids and amino acid

173   levels) for up to 4 fold changes of each of the macronutrient in plasma. These metabolite

174   combinations were used as a proxy for the dietary macronutrient input to system (i.e.

175   combinations of low, medium, high and very high levels of carbohydrates (~glucose), proteins

176   (~amino acids) and fats (~fatty acids) in diet). The effects of these macronutrients were recorded

177   through the MFD (metabolic flux distribution) in the hepatic metabolic pathways. The

178   representative MFD for the constant plasma macronutrient levels with high carbohydrate and

179   protein with normal fat levels is shown in Fig. 3. The figure shows that under such a scenario,

180   the fatty acid and cholesterol synthesis increase despite the normal dietary fat consumption. The

181   lipogenesis flux is strongly activated under such a condition. These results are also in line with

182   the experimental observationsfor the high carbohydrate diet in hamsters(47). However, for a

183   scenario wherein the plasma fatty acids levels are higher with normal carbohydrates and amino

184   acids, the MFD show a increase in the gluconeogenesis flux with decreased fatty acid synthesis

185   (See Fig.4). The increase in gluconeogenesis under high fat diet has been experimentally

186   confirmed in rats (9). This analysishighlights the non-linear dependence of metabolic fluxes with

187   respect to the plasma macronutrient levels. Such a metabolic flux distribution was used to obtain

188   the fold change in the individual flux value relative to that observed under physiological resting

189   state. We discuss the effect of macronutrient level on the fluxes through the fold change values

190   in various metabolic reactions.
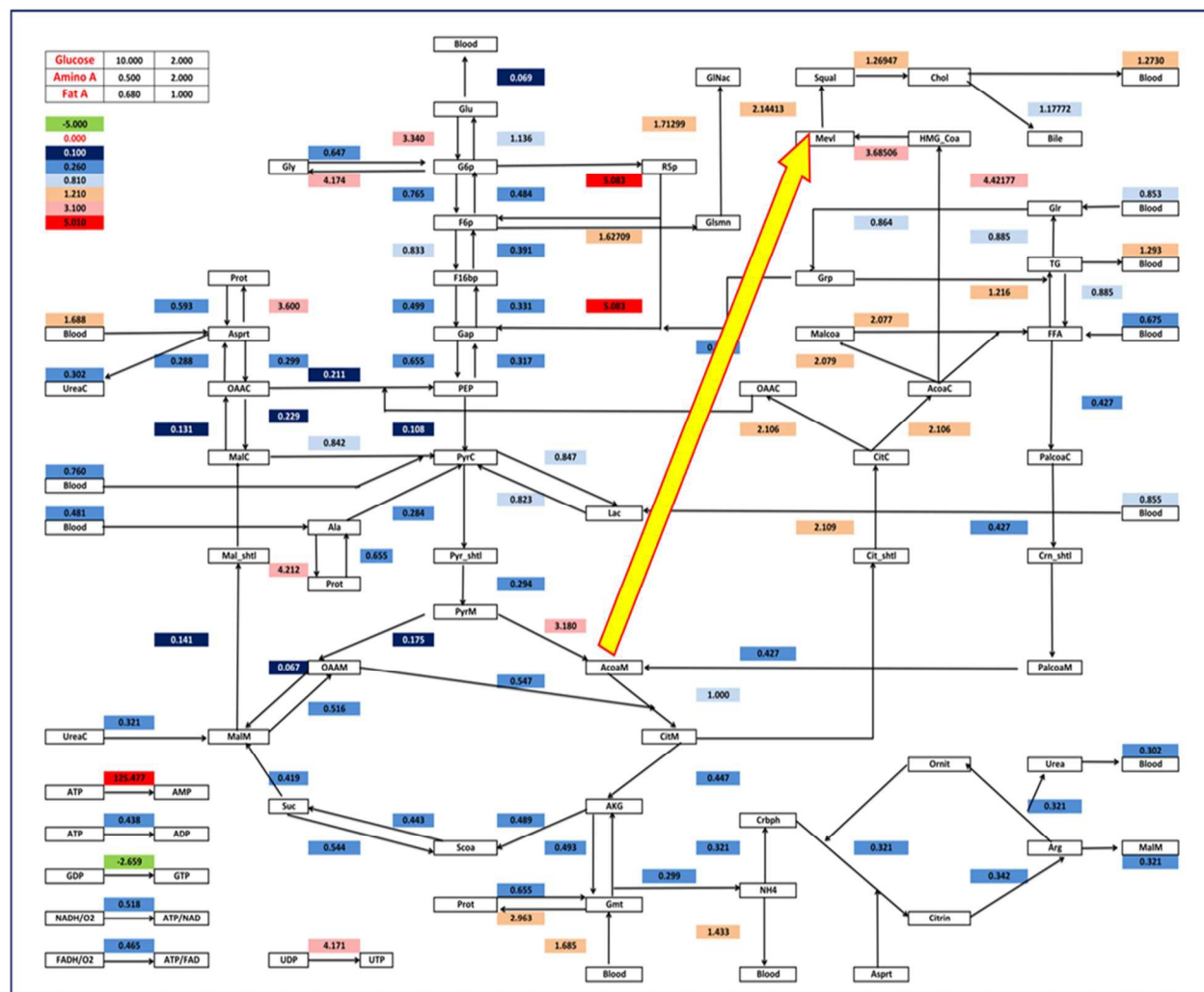
191

192   **Figure 3** The metabolic flux distribution for the scenario where the plasma glucose is set to 10

193   mmol/l, plasma amino acid are set to 0.5mmol/l and fatty acids set to 0.68 mmol/l. This

194   represents the diet with high carbohydrates and protein with normal fat content. The yellow

195   arrow shows the diversion of the metabolic flux towards the lipogenesis.The color code represent

11

196 the fold change -green to colorless for negative fold change to zero(<=0), colorless to blue for

197 zero to one (0-1) and blue to red for one to greater than one (1 to >1).

198
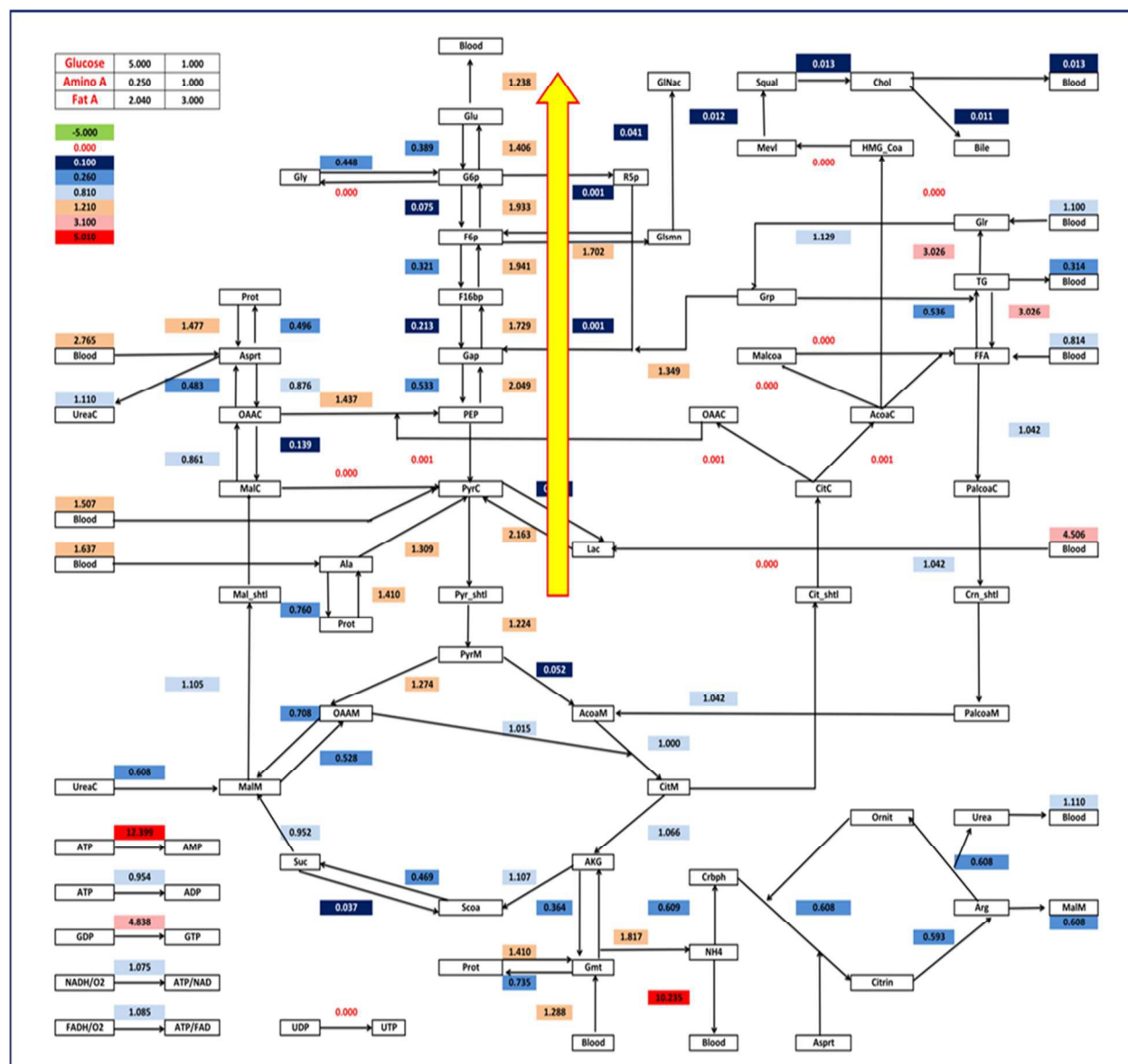
199

200 **Figure 4** The metabolic flux distribution for the scenario where the plasma glucose is set to 5

201 mmol/l, plasma amino acid is set to 0.25 mmol/l and fatty acids set to 2.4 mmol/l. This

202 represents the diet with normal carbohydrates and protein with high fat content. The yellow

203 arrow represents the diversion of the metabolic flux towards gluconeogenesis.The color code

204   represent the fold change -green to colorless for negative fold change to zero(<=0), colorless to

205   blue for zero to one (0-1) and blue to red for one to greater than one (1 to >1).

206   We furtherused the model to study the intracellular metabolic flux variations with respect to the

207   different combination of plasma macronutrient levels. The diet combinations involved variations

208   in plasma amino acids and plasma fatty acid concentrations for different plasma glucose levels,

209   namely, low (3mM), normal (5mM), high (10 mM) and very high (15mM Henceforth we denote

210   the plasma concentrations of macronutrients on the scale of low to very high levels. Table I

211   represents the concentrations and fold change values for each of the macronutrient

212   correspondingly to the scale of low to very high level.

213   **Table I**: The different levels of macronutrient and the corresponding physiological

214   concentrations used during simulation.

Macronutrient/ Level	Normal/ Ref mmol	Low mmol	Medium mmol	High mmol	Very high mmol
Glucose	5	<5 < 1 fold	5-8 1-1.6 fold	8-12.5 1.6-2.5 fold	>12 >2.5 fold
Fatty acids	0.68	<0.68 < 1 fold	0.68-1.36 1-2 fold	1.36-2.04 2-3 fold	>2.04 >3 fold
Amino acids	0.25	<0.25 < 1 fold	0.25-0.5 1-2 fold	0.5-0.75 2-3 fold	>0.75 >3 fold

215

Gluconeogenesis and Glycolysis

217   First, we present the effect of diet on glucose synthesis/ assimilation by characterizing the

218   gluconeogenesis/ glycolysis fluxes. To address the glucose metabolism, the net steady state flux

219   response around the substrate cycles in the pathway were recorded (48). The flux differences at

220   the irreversible steps in the glycolytic pathway were recorded to characterize the net flux towards

221   gluconeogenesis and glycolysis. In this case, the flux value around the reversible reaction F6p to

222 F16bp was recorded by normalizing the difference in flux through fructose 1,6, biphosphatase

223 (gluconeogenesis) and phosphofructo kinase (glycolysis) (See Fig.5). In the figure, the value of 1

224 on the color bar represents the normalized value of the difference in the gluconeogenesis and

225 glycolysis flux (normalized by the basal difference in the flux). As expected, gluconeogenesis is

226 preferred for both low and normal glucose condition irrespective of the amino acid and fatty acid

227 levels. High gluconeogenesis flux can be observed even under normal glucose condition but with

228 a very high fatty acid levels. Glycolysis is dominant on increasing the plasma glucose levels at

229 high amino acids-low fatty acids and low amino acids-high fatty acidlevels.

230 A similar trend is reflected in the Glucose to G6p (glucose 6 phosphate) and G6p to Glucose flux

231 as observed in Fig 6. It shows the normalized difference of the flux through glucose 6

232 phospahatase (gluconeogenesis) and glucokinase (glycolysis).The GK (glucokinase) flux

233 increases with increasing glucose levels, whereas, G6pase flux increases with decreasing plasma

234 glucose concentrations. However at higher glucose levels, GK flux is overcome by G6pase at

235 higher amino andfatty acidlevels.

236 Under very high fatty acid and amino acid levels, gluconeogenesis is dominant over glycolysis

237 indicating higher glucose release into the plasma. This is also reflected by plotting the glucose

238 transport flux into the plasma, wherein high glucose release is observed under low plasma

239 glucose condition and under high amino acid and high fatty acid levels (See Fig. 7). This is

240 mainly due to the inhibition of AKT (protein kinase B), a glycolytic regulator, and activation of

241 PKA that triggers gluconeogenesis under such conditions(See S1 file Fig.N1 and N2). The

242 inhibition of AKT at higher fatty acid levels even under high glucose levels is due to the over

243 activation of PKC (protein kinase C) which has a negative feedback on AKT phosphorylation(S1

244 file Fig. N3). It can be noted that under moderately high glucose levels, low amino acid and high

245   fatty acid levels results in an efficient glucose uptake (i.e. no release). This may be significant

246   under transient condition during food intake, where the plasma glucose levels rise to moderately

247   high levels.

248
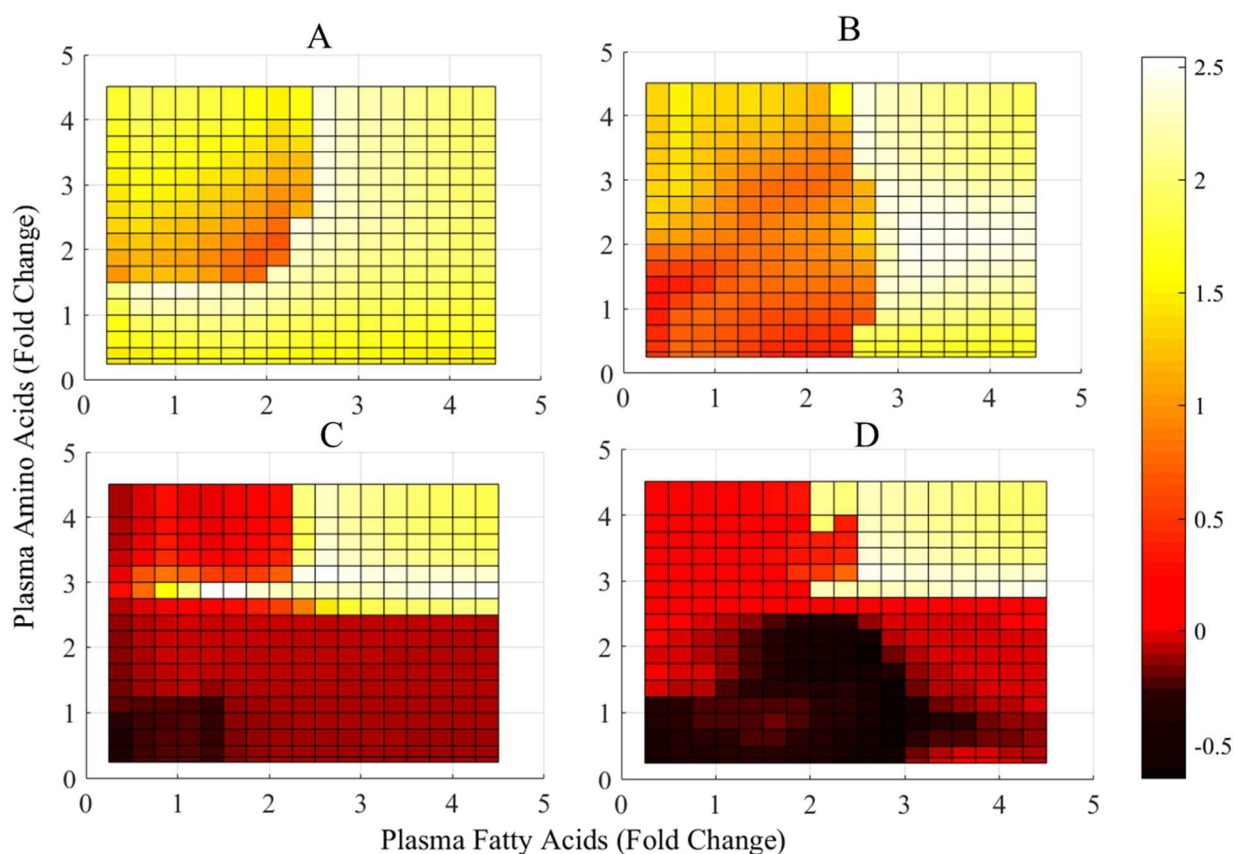
249

250   **Figure 5** Thegraph represents the normalized difference in the gluconeogenesis (F16bpase flux)

251   and glycolysis (PFK flux) for the F61bp to F6p and F6p to F16bp flux, respectively, for varying

252   foldsof plasma amino and fatty acids for four different glucose levels. A positive value on the

253   color bar represents the prevalence of gluconeogenesis and a negative value represents the net

254   flux to be as glycolysis. The subplots A, B, C & D represents the flux variations for plasma

255   glucose concentration of 3mM, 5 mM, 10 mM and 15 mM,respectively.Gluconeogenesis

256   (F16bpase flux) increases with decreasing glucose levels and increasing amino-fat levels.

15

257 However, with increasing glucose levels, gluconeogenesis further decreases with increasing fat

258 levels under moderate amino acid levels. Glycolysis (PFK flux) increases with increasing

259 glucose levels and decreasing fat levels. However at higher glucose levels the trend becomes

260 nonlinear with fat and amino acids. At very high glucose levels, glycolysis is higher at either

261 very low to moderate amino-fatty acid levels. It is mostly inhibited at very high amino-fat levels.
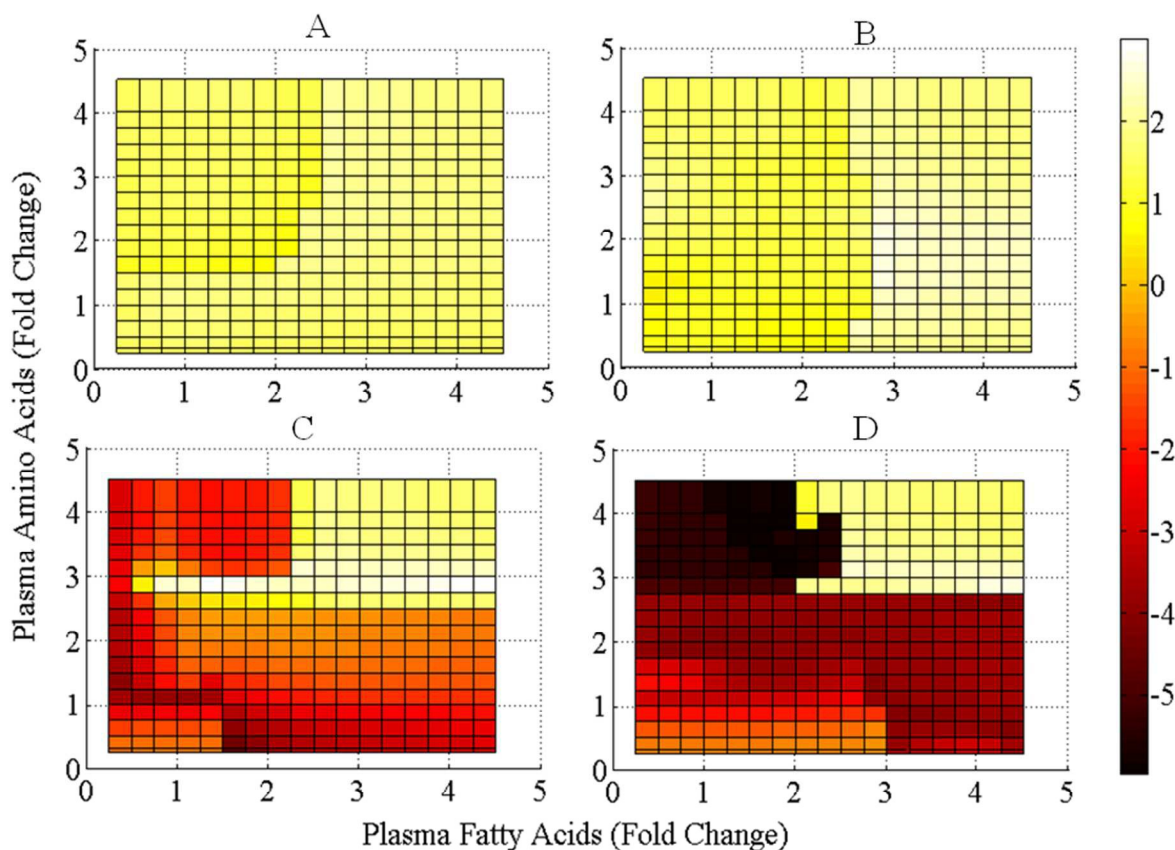
262

263 **Figure 6** The normalized difference in the gluconeogenesis (Glucose 6 phosphatase flux-

264 G6pase) and glycolysis (Glucokinase flux-GK) for the G6p to Glucose and Glucose to G6p flux,

265 respectively, for varying levels of plasma amino and fatty acids for four different glucose levels.

266 A positive value on the color bar represents the prevalence of gluconeogenesis and a negative

267 value represents the net flux to be as glycolysis. The subplots A, B, C & D represents the flux

268 variations for plasma glucose concentration of   3mM, 5 mM, 10 mM and 15 mM,

269   respectively.The GK flux increases with increasing glucose levels, whereas, G6pase flux

270   increases with decreasing glucose concentrations. However at higher glucose levels, GK flux is

271   overcome by G6pase at higher amino-fat levels. The GK flux is highest at high glucose-amino

272   and low fat levels.
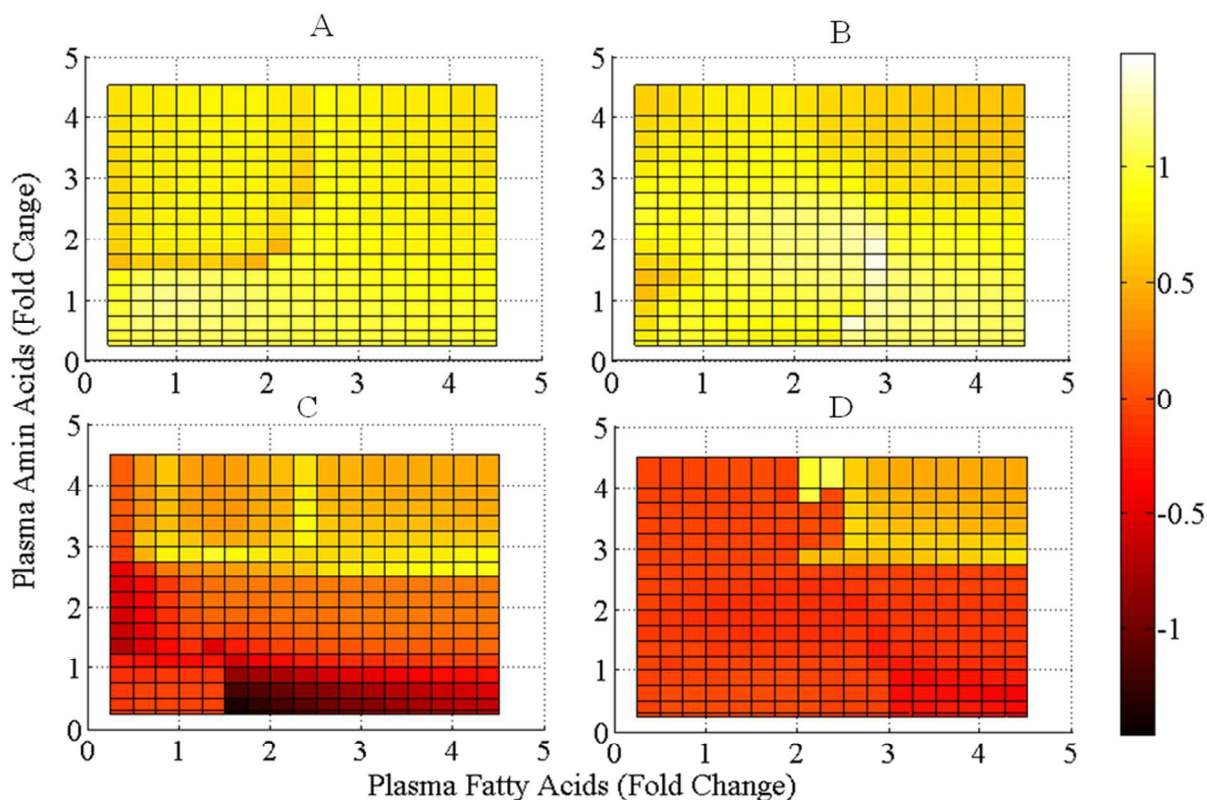
273

274   **Figure 7** The glucose transport flux for varying levels of plasma amino and fatty acids for four

275   different glucose levels. A positive value on the color bar represents the glucose release into the

276   plasma from the liver, whereas a negative value represents the uptake of the glucose by hepatic

277   tissues.The subplots A, B, C & D represents the flux variations for plasma glucose concentration

278   of 3mM, 5 mM, 10 mM and 15 mM, respectively. Glucose release increases with decreasing

279   glucose concentration in blood and vice-versa. However, under higher glucose levels, glucose

280 uptake increases at high fat and moderate amino acid levels. Under higher glucose levels,

281 glucose release increases with higher amino and fatty acid levels.

282 The glycolytic flux through PFK (phosphofructokinase) in the pathway (downward flux towards

283 pyruvate) is plotted in Figure 8. In this case, under normal glucose, amino acids and fatty acid

284 levels, the glycolysis is partially active with gluconeogenesis also operational indicating that

285 gluconeogenesis is being accounted for by glycogen breakdown, while some of the flux

286 contributes to the energy requirements of the liver. It can be distinctively noted that the PFK flux

287 increases with increasing amino acid levels under low to moderately high glucose levels and

288 moderate fatty acid levels. This increase in glycolytic flux indicates the saturation of glycogen

289 levels and the flux is directed towards pyruvate. However, under very high glucose levels, the

290 glycolytic flux is highest either at low fatty and amino acid or moderate amino acid and high

291 fatty acid levels (See Fig. 8D).
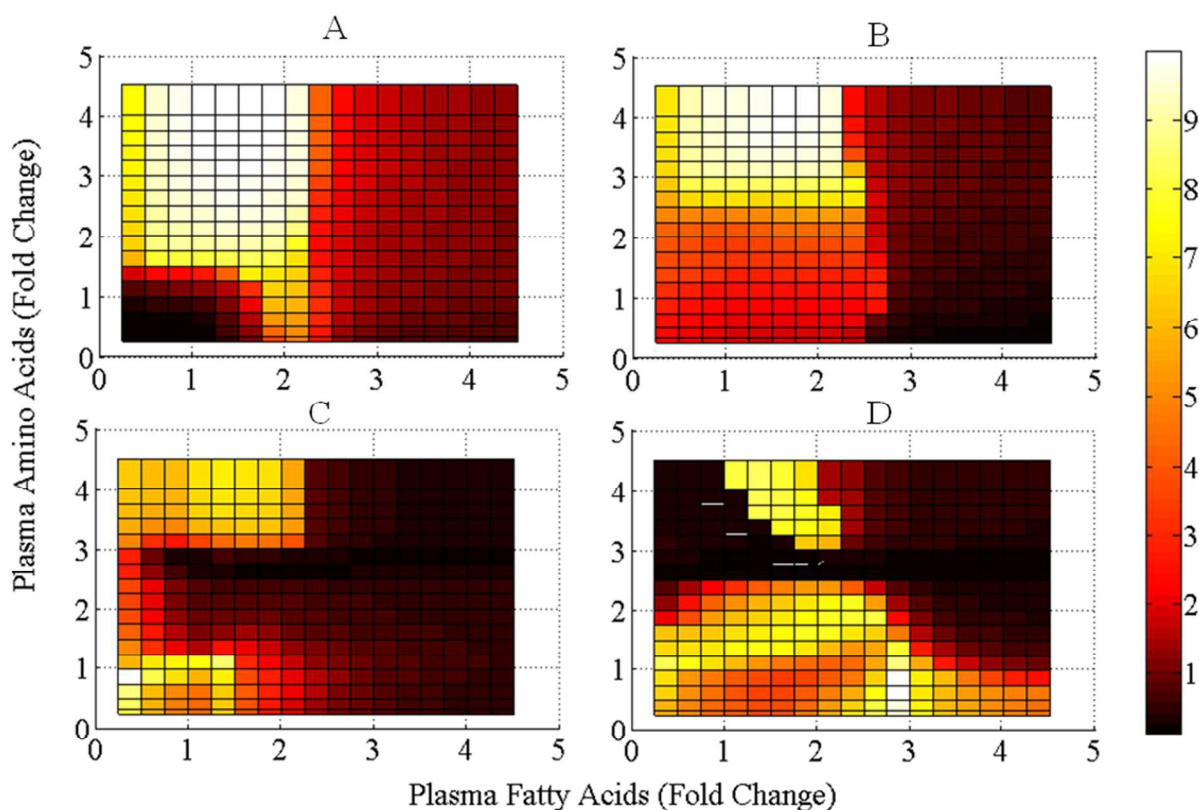
292

293   **Figure 8** Thephosphofructokinase flux (PFK), for varying levels of plasma amino and fatty

294   acids for four different glucose levels. The subplots A, B, C & D represents the flux variations

295   for plasma glucose concentration of 3mM, 5 mM, 10 mM and 15 mM,respectively.PFK flux

296   increases with increasing glucose levels and decreasing fat levels. However, at higher glucose

297   levels the trend becomes nonlinear with fat and amino acids. At very high glucose levels, it is

298   higher at either very low or very high amino acid levels. It is mostly inhibited at very high

299   amino and fatty acid levels.

300   **Glycogen Metabolism**

301   The metabolic process that affects glucose synthesis and storage is glycogen metabolism. The

302   glycogen metabolism is characterized by plotting the normalized difference between the flux

303   through Glycogen phosphorylase (glycogen breakdown) and Glycogen synthase (glycogen

304   synthase), which catalyzes G6p to glycogen and glycogen to G6p reactions, respectively (See

305   Fig.9). The glycogen catabolic flux (i.e. glycogen breakdown) shows a similar trend as

306   gluconeogenesis. Under low glucose levels, the glycogen breakdown is reduced under high fat

307   levels which may result in lower glucose supply to the plasma.
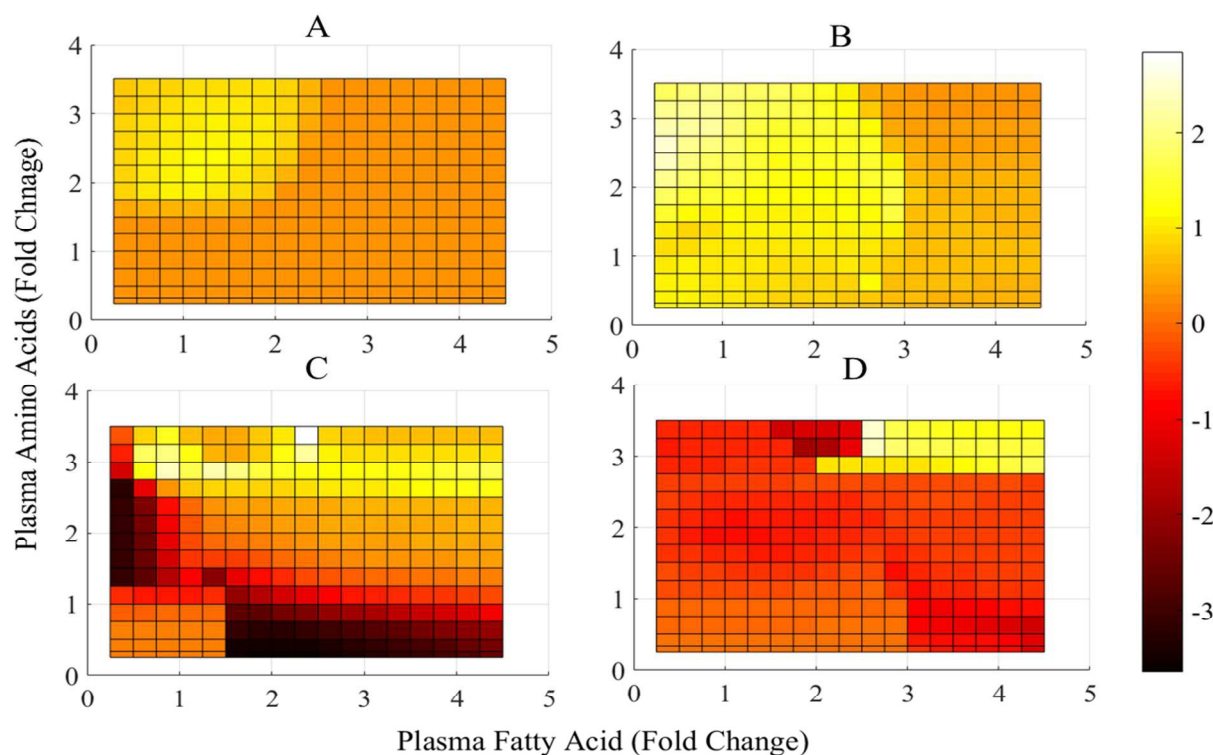
308

309 **Figure 9** Thedifference in the glycogenolysis (Glycogen phosphorylase) and glycogen synthesis

310 (Glycogen synthesis) for the G6p to Glycogen and Glycogen to G6p flux, respectively varying

311 levels of plasma amino and fatty acids for four different glucose levels. A positive value on the

312 color bar represents the prevalence of glycogen breakdown and a negative value represents the

313 net flux towards glycogen synthesis. The subplots A, B, C & D represents the flux variations

314 for plasma glucose concentration of 3mM, 5 mM, 10 mM and 15 mM, respectively.Glycogen

315 synthesis increases with increasing glucose concentration and decreases with increasing fat and

316 amino acids for normal glucose levels. However at very high glucose levels, it increases with

317 increasing amino acid levels provided that fat levels are moderate. It is reduced at high amino

318 and fatty acidlevels and at low amino acid and high glucose levels. Glycogen breakdown

319 increases with decreasing glucose levels and increasing amino and fatty acid levels.

320   The glycogen synthesis is highest under moderately high glucose with either low fatty acid - high

321   amino acid or high fatty acid-low amino acid levels. This can be due to higher activation of

322   AMPK which inhibits glycogen synthesis under such condition (See supplementary file II-

323   Fig.S4). Under very high glucose levels glycogen synthesis is not as efficient as that under

324   moderate glucose levels. The signaling molecule regulating the glycogen metabolism (i.e.

325   phosphorylated GSK3 (inactive) helps in glycogen synthesis) is also shown inFigure 10. It can

326   be seen that irrespective of the glucose levels, GSK3p is inhibited strongly at very high amino

327   and fatty acid levels in the plasma, whereas it is highest under low amino and fatty acid condition

328   for moderately high glucose levels. Under very high glucose levels, GSK3p is highest (almost 10

329   folds) for all the levels of fatty acid and amino acids, except high fatty and high amino acid

330   levels due to inhibition of insulin signaling at very high amino and fatty acids.
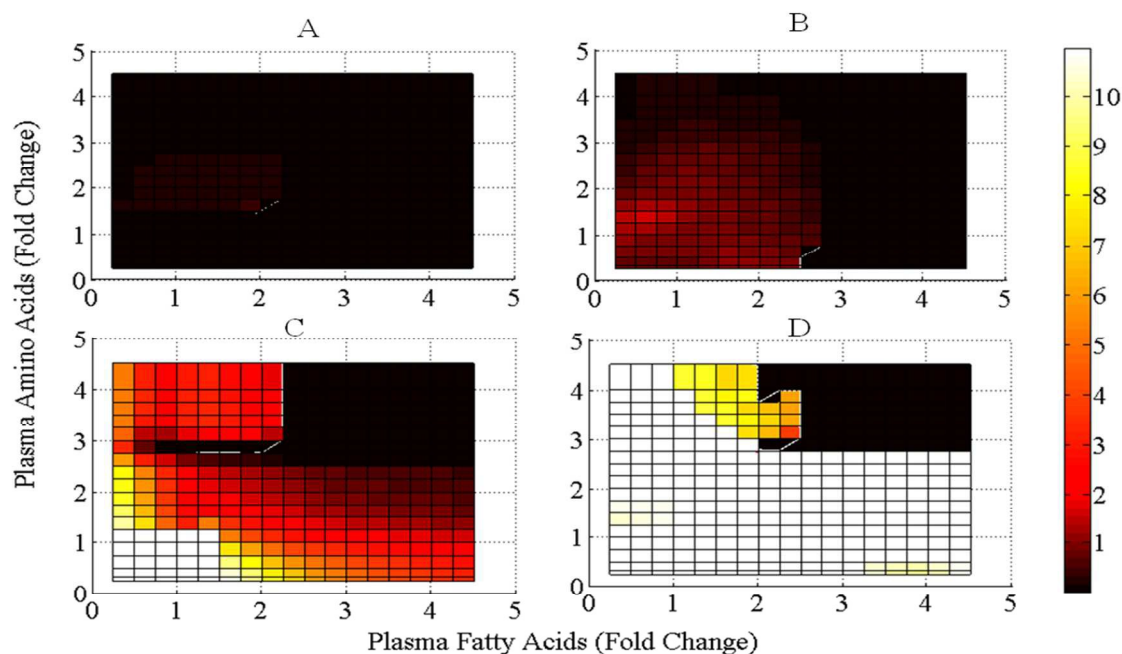
331

332   **Figure 10** Thelevels of phosphorylated Glycogen synthase kinase (GSK3), varying levels of

333   plasma amino and fatty acids for four different glucose levels. The subplots A, B, C & D

334   represents the flux variations for plasma glucose concentration of 3mM, 5 mM, 10 mM and 15

335   mM,respectively. The phosphorylation of Glycogen synthase kinase increases with increasing

336   glucose levels and decreases with increasing amino and fatty acid levels. It is mostly inhibited at

337   high amino-fatty acid levels.

338   **Pyruvate and Lactate Metabolism**

339   The trends observed in the glycolysis flux are also directly reflected in the pyruvate uptake from

340   plasma, wherein the uptake of pyruvate is low under higher glycolytic conditions (S1 file

341   Fig.M3). Moreover, pyruvate is released under higher glycolysis conditions, wherein the PFK to

342   F16bpase flux difference is highest as noted in Fig.5 (darker regions in the plots). While

343   pyruvate uptake is high under low glucose levels, the pyruvate release increases at very high

344   amino acid glucose levels under low fat levels due to its higher synthesis rate. This indicates that

345   the accumulation of carbon from high glucose is mainly channeled towards fatty acid synthesis.

346   In liver, pyruvate is also synthesized from alanine and lactate under normal physiological

347   conditions,whereas, under excessive pyruvate production, the fate of pyruvate can be towards

348   lactate through lactate dehydrogenase. The figure shows the normalized difference of the

349   pyruvate to lactate reversible flux, wherein the positive flux represents the net flux towards

350   pyruvate formation and the negative value represents the net flux towards lactate formation (See

351   Fig.11). The lactate to pyruvate flux is reduced for low glucose levels only under moderate to

352   high amino acid and low fatty acid levels, thereby reducing the efficiency of gluconeogenesis as

353   reflected in Fig.5. This is also reflected in the trendsof NADH/NAD ratio (nicotinamide adenine

354   dinucleotide) under these conditions. Whereas pyruvate synthesis increases with increasing fatty

355   acid levels under lower and normal glucose levels.

356   However, under higher glucose levels lactate synthesis is favored with increasing fatty acid

357   concentrations under moderate amino acid levels. This increase in lactate flux is due to higher

358   pyruvate synthesis from its glycolytic precursors and the favorable NADH/NAD ratio under the

359   conditions of high glucose and fatty acid levels(See Fig. 12). Similar trend is further reflected in

360   the lactate transport flux, wherein higher lactate uptake is associated with increased flux towards

361   pyruvate synthesis and vice versa (See S1 file Fig.M4). Moreover, the flux through pyruvate

362   carboxylase which catalyzes pyruvate to oxaloacetate (See Fig.13) follows the similar trend as of

363   depicted by the gluconeogenesis flux and lactate dehydrogenase flux (Fig.5 & Fig.11). This flux

364   utilizes partial TCA cycle, wherein the pyruvate is reutilized for the gluconeogenesis. This flux

365   also facilitates the utilization of alanine and lactate as the substrates for gluconeogenesis through

366   pyruvate. Under high glucose, amino and fatty acid levels, both lactate dehydrogenase and

367   pyruvate carboxylase fluxes are higher. This indicates that the competition between these two

368   fluxes decides the major fate of pyruvate (i.e. glucose or lactate) under these conditions (See

369   Fig.11D &S1 file Fig.M5 (D)).
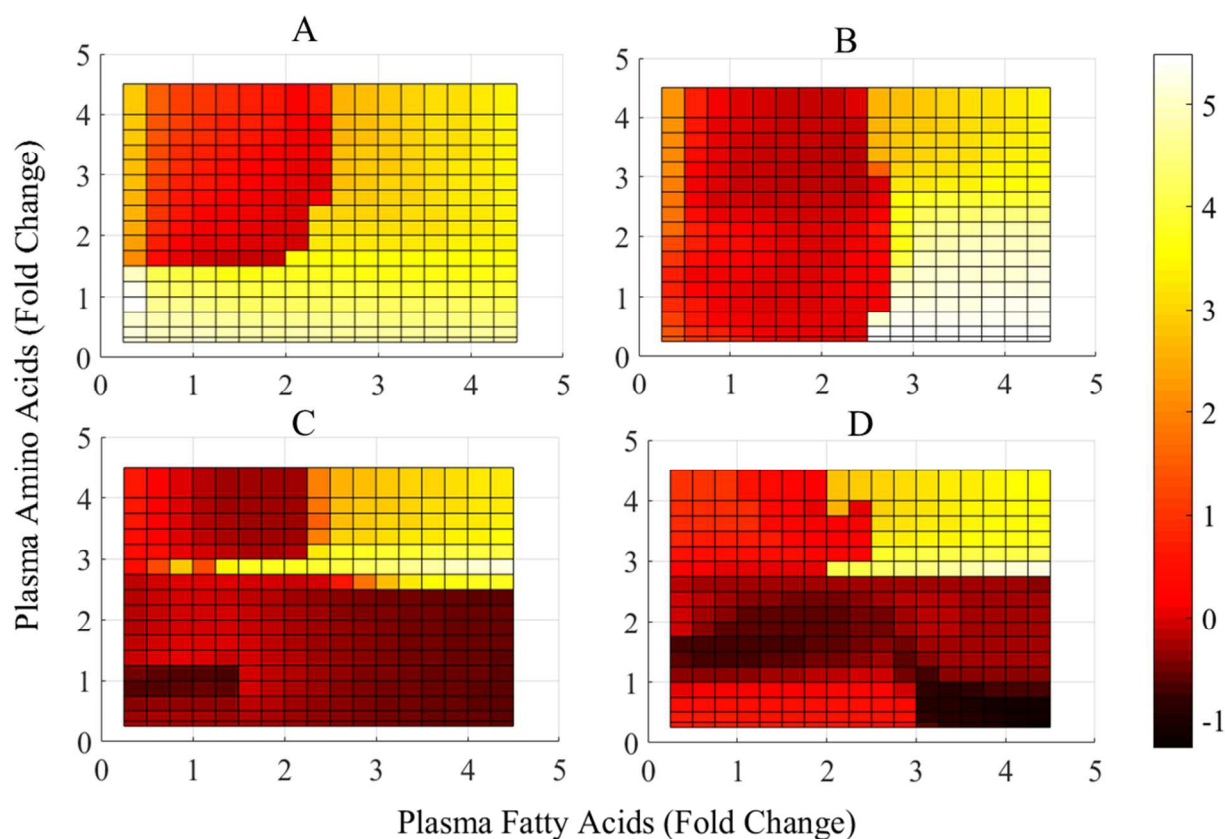
Figure 11 Thereversible lactate dehydrogenase flux for varying levels of plasma amino and fatty acids for four different glucose levels. A positive value on the color bar represents the lactate to pyruvate flux, whereas a negative value represents the pyruvate to lactate flux.The subplots A, B, C & D represents the flux variations for plasma glucose concentration of 3mM, 5 mM, 10 mM and 15 mM, respectively.Pyruvate synthesis increases with increasing fatty acid levels for lower and normal glucose levels. However under higher glucose levels, lactate synthesis is favored with increasing fatty acid levelsfor medium amino acid levels.

379
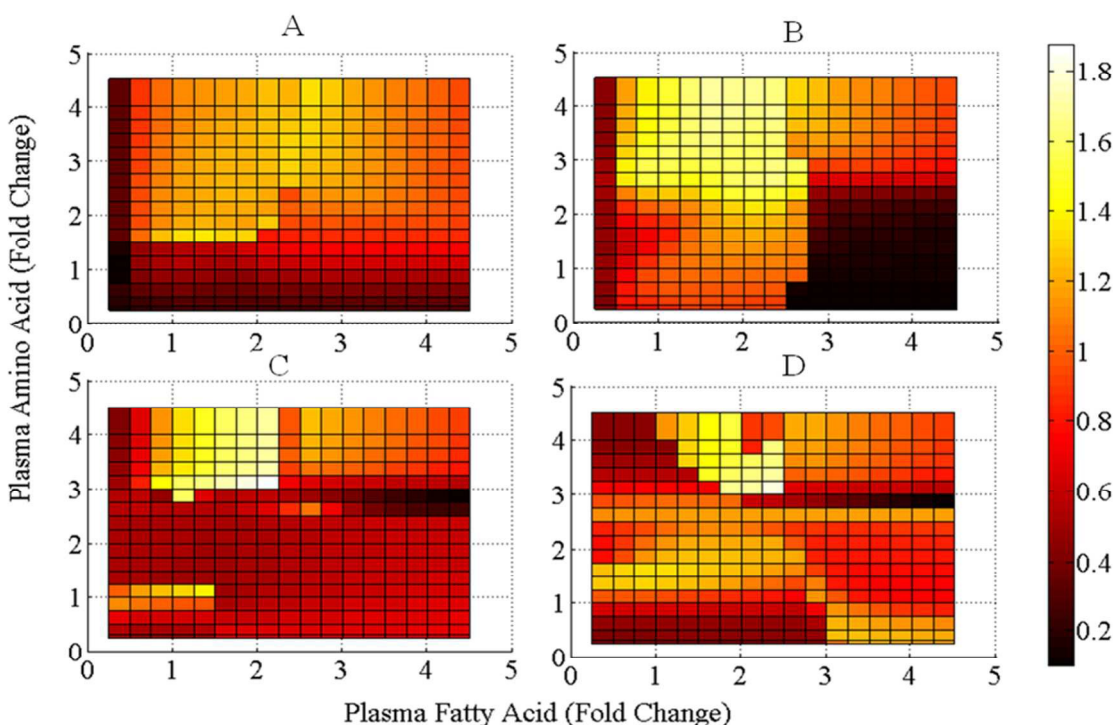
Figure 12 TheNADH/NAD ratio for varying levels of plasma amino and fatty acids for four

different glucose levels. The subplots A, B, C & D represents the flux variations for plasma

glucose concentration of 3mM, 5 mM, 10 mM and 15 mM,respectively.The NADH/NAD ratio

increases with increasing amino acid levels and decreases with increasing fatty acid levels for

normal glucose levels. With increasing glucose levels the ratio decreases slightly and is nonlinear

with amino acid and fatty acid levels. However, under high glucose levels, higher levels of

amino and fatty acids can restore normal ratio.

TCA Cycle and ATP-ADP ratio

Flux towards TCA cycle is an indicator of the ATP (adenosine triphosphate)and fatty acid

synthesis. Here, the TCA flux is indicated by pyruvate dehydrogenase flux that catalyzes

pyruvate to acetyl-coA. The TCA flux is low forlow glucose level when gluconeogenesis is

prevalent (See Fig.13). However, under normal glucose levels, only under high fatty acid levels

the TCA flux is reduced (See Fig.13B).On further increasing glucose, TCA cycle is most

393   preferred at low fat high amino acid levels, and strongly inhibited under high amino acid high

394   fatty acid levels. The flux from pyruvate to AcoA (acetyl coenzyme A) is an amphibolic flux,

395   being activated by insulin and glucagon signaling, thereby influences both anabolic and catabolic

396   process. The flux is high through glucagon signaling activation under high amino and fatty acid

397   levels (indicating catabolism), while it is high through insulin signaling activation under high

398   glucose high fatty acid levels (indicating anabolism). Further, to characterize the energy status of

399   the liver with respect to dietary macronutrient composition, we plotted the ratio of the ATP

400   breakdown to ATP production rates, which is denoted by adenylate kinase and oxidative

401   phosphorylation flux, respectively (SeeS1 file Fig. M6). Subsequently, we also plotted the

402   resulting ATP/ADP ratio (See Fig.14).
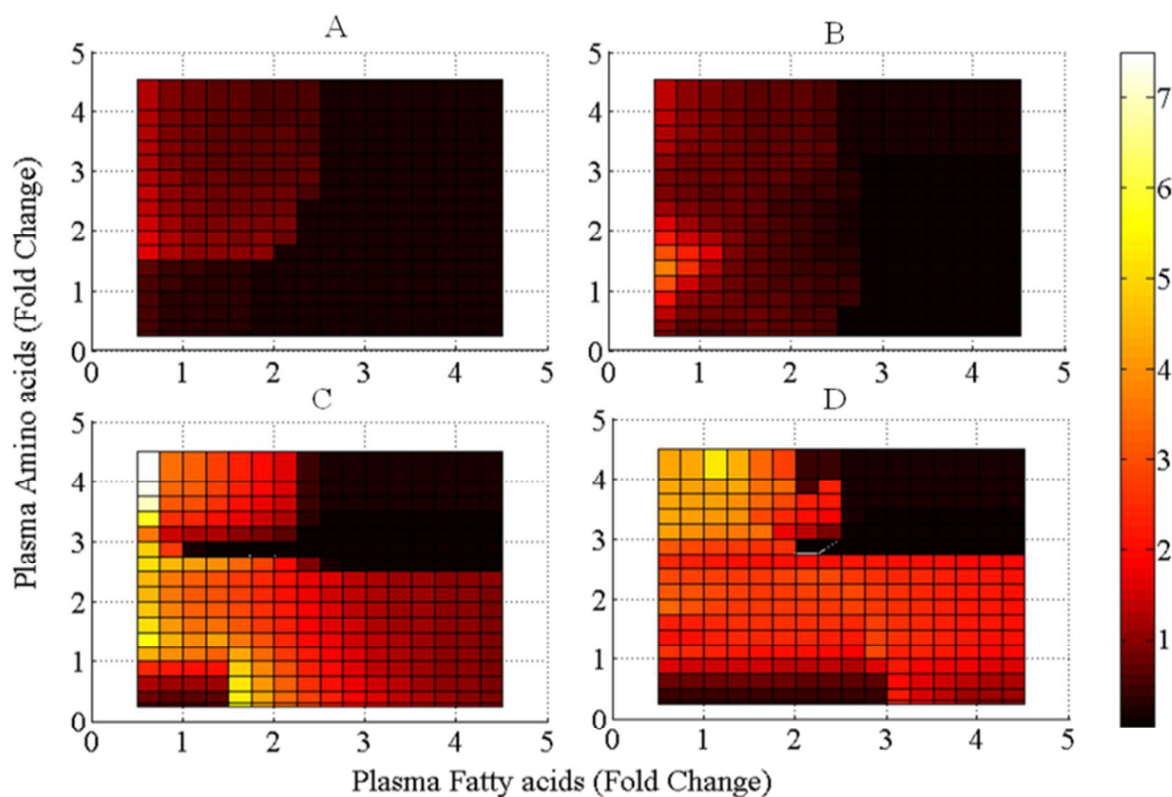
404   **Figure 13** Thepyruvate dehydrogenase flux for varying levels of plasma amino and fatty acids

405   for four different glucose levels. The subplots A, B, C & D represents the flux variations for

406 plasma glucose concentration of 3mM, 5 mM, 10 mM and 15 mM, respectively.The pyruvate

407 dehydrogenase flux increases with increasing amino acid level and decreases with higher fatty

408 acid levels for all glucose levels. However the flux increases monotonously with increasing

409 glucose concentration and is inhibited at very high fatty and amino acid levels.

410 The energy utilization is higher under low glucose levels, indicating that in liver the energy is

411 being utilized for the gluconeogenesis. This is evident from the supplementary file S1 Figure

412 M6(A) and Figure 14(A), that under low glucose levels, while ATP breakdown is higher, the

413 ATP/ADP ratio is lower indicating increase in ADP (adenosine diphosphate) levels. However,

414 on increasing glucose levels, under moderate amino acid levels, ATP synthesis dominates under

415 most levels of fatty acids (the ratio is less than one in supplementary file II-Fig.M6 (C&D)). It is

416 interestingto observe that under high fat high amino acid levels, the ATP synthesis is low

417 indicating a reduced drive towardsanabolic reactions. This is also reflected in ATP/ADP ratio,

418 under low glucose concentrations where gluconeogenesis dominates (SeeS1 file Fig.M6A).

419 Under normal glucose concentrations and high amino acid levels the ATP/ADP ratio is lower

420 indicating catabolic effect (Fig. 14B). However under low amino acid levels, the ATP/ADP ratio

421 is near normal under all conditions. On increasing glucose(moderately high), the ATP/ADP ratio

422 drops in most cases, except under moderate amino acid and high fatty acid levels. On further

423 increasing the glucose (very high), it can be seen that ADP dominates with deficient ATP

424 indicating abnormal anabolic conditions (See Fig.14D). This is due to lower oxidative

425 phosphorylation caused by higher insulin which inhibits PKA and calcium i.e. regulators of

426 oxidative phosphorylation. The lower oxidative phosphorylation under high glucose levelsis also

427 accompanied by the higher ATP consumption due to anabolic condition resulting into the steep

428 fall in the ATP/ADP ratio.

Pentose Phosphate Pathway

429

430 Next we consider the flux towards pentose phosphate pathway indicating the degree of anabolic

431 reactions (biosynthesis) and the measure for the supply of redox equivalent (NADPH). This flux

432 is represented by the rate of the flux through G6p dehydrogenase (abstracted for conversion of

433 G6p to R5p) (See S1 file Fig. M7). As expected, the pentose phosphate pathway is off at low

434 glucose levels irrespective of the amino and fatty acid levels. However it is reduced at higher fat

435 levels fornormal glucose levels. Under normal glucose levels, the pentose phosphate pathway is

436 operational under basal levels. The maximum pentose phosphate pathway flux is observed under

437 moderately high glucose and amino acid levels. Further at very high glucose, pentose pathway is

438 operational at basal levels for moderate amino acid and high fatty acid levels. The pentose flux is

439 inhibited at high amino and fattyacid levels. At very higher glucose levels, pentose flux is

440 functional either at moderate amino acid levels or low to moderate amino acids and high fat

441 levels (See S1 file Fig.M7 (D)). Moreover, in S1 file Fig. M7 (D), the operational region of

442 pentose phosphateflux) maps the conditions where the F16bpase and PFK fluxes are highly

443 reduced, which implies the diversion of the flux towards pentose phosphate pathway under such

444 dietary conditions. Such response enhances lipogenesis by providing more reducing equivalents

445 under high fatty acids and higher glucose levels.
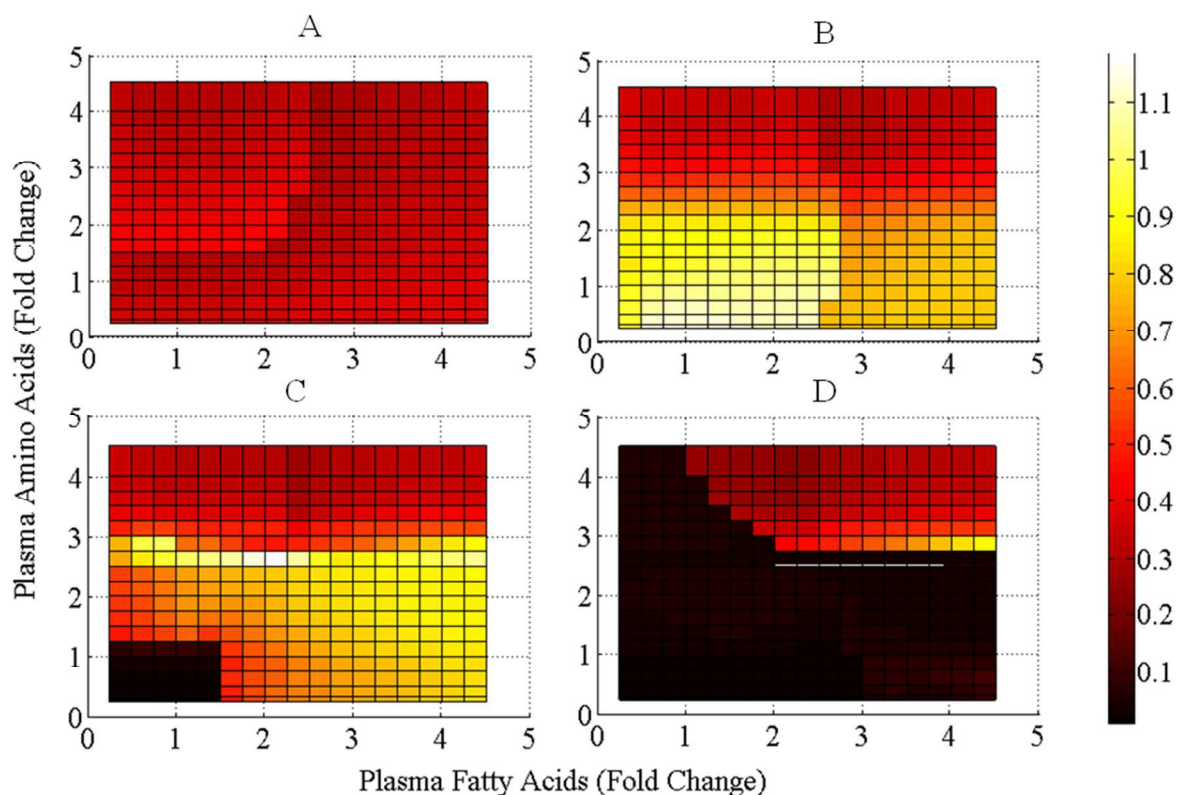
446

447   **Figure 14**   TheATP/ADP ratio for varying levels of plasma amino and fatty acids for four

448   different glucose levels. The ratio above one represents the net surplus of ATP over ADP.The

449   subplots A, B, C & D represents the flux variations for plasma glucose concentration of 3mM, 5

450   mM, 10 mM and 15 mM, respectively.The ATP/ADP ratio is maintained at normal under normal

451   glucose and moderate amino-fatty acid levels. The ratio decreases with decreasing glucose levels

452   below normal. However,for higher glucose levels, high level of fatty acids is required to

453   maintain the normal ratio. The ratio decreases with higher amino acid levels forhigh glucose

454   levels. The ratio is drastically reduced at very high glucose and fatty acid levels.

455

456   **Fat Metabolism**

457   We next consider the flux towards lipogenesis (i.e. fatty acid and triglyceride synthesis). We

458   firstly quantify the fatty acid synthesis by characterizing the flux through Acetyl-coA to

459   Malonyl-CoA catalyzed by Acetyl-coA carboxylase (ACC)(See S1 file Fig.M7). Under low

460   glucose levels, due to higher gluconeogenesis, lipogenesis is minimal forall levels of amino acid

461   and fatty acids. Under normal glucose level, there is an enhanced lipogenesis, albeit at normal

462   level under normal fatty and amino acid levels. On increasing glucose concentration further, the

463   maximum lipogenesis is observed and is seen for moderate amino acid low fatty acid and

464   moderate fatty acid low amino acid levels. It can be noted that, forvery high plasma glucose

465   levels, the lipogenic flux is operational in the region where the pentose phosphate pathway is

466   also active (See S1 file Fig.M7(D) and Fig. 15(D)). However, at higher glucose levels, both

467   under low amino acid/low fatty acid and high amino acid / high fatty acid, the lipogenesis is

468   completely inhibited which is due to lower levels of ATP levels countering the lipogenesis (an

469   anabolic process). This is also associated with the state of the lipogenic regulators(49), wherein

470   CHREBp(carbohydrate response element binding protein)an activator of lipogenesis increases

471   with glucose and inhibited by higher fatty acids and amino acids due to activation of AMPK

472   (AMP activated protein kinase) (an inhibitor of CHREBP) under such conditions (See S1 file

473   Fig.N5). TRB3 (Tribbles homolog 3) is an inhibitor of lipogenesis (See Fig.N6) is activated at

474   high fatty acid under normal glucose level, which inhibits AKT activity that is required for

475   lipogenesis.

476   The triglyceride metabolic flux is characterized by the flux ratio for triglyceride synthesis to

477   triglyceride breakdown (See Fig. 16). The triglyceride synthesis is low, as expected, under low

478   glucose levels irrespective of the dietary amino and fatty acid levels. Under normal glucose

479   levels, its synthesis is high under moderate fatty/amino acid levels. The triglyceride synthesis

480   space increases on further increasing glucose, with high synthesis rates noted for low to

481   moderate amino acid and high fatty acid levels. The triglyceride synthesis is activated by

482   PPARγ(Peroxisome proliferator-activated receptor gamma), which in turn is activated by insulin

483   and fatty acids (See S1 file Fig. N7). This helps in the anabolic accumulation of triglycerides in

484   the liver under these conditions. However, for very high glucose level, the system limits ATP for

485   anabolic reactions to happen thereby reducing triglyceride synthesis. Although PPARγ is

486   activated at higher fatty acid levels, AKT is inhibited due to activation of FOXO (forkhead box

487   protein) which is operational under high fatty acid levels (See S1 file Fig. N8). Moreover, the

488   activation of PPARα under very high fatty acid levels induces triglyceride and fatty acid

489   breakdown thereby reducing lipogenesis (See S1 file Fig.S9). The triglyceride release into the

490   blood also mimics a similar behavior as that of its synthesis (See S1 file Fig.M8).
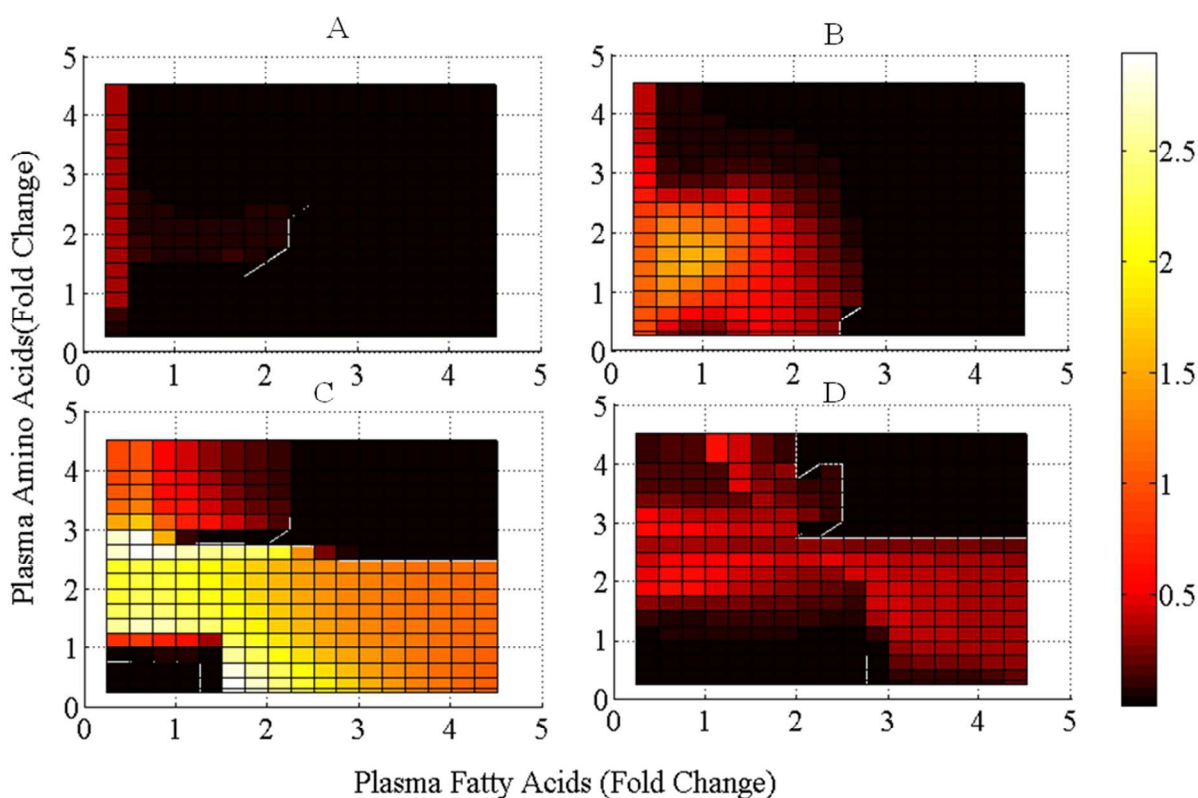
491

492   **Figure 15** Theflux through lipogenesis [fatty acid synthesis] represented by Acetyl CoA

493   carboxylase (ACC)flux that catalyzes Acoa to MalonylCoaA for varying levels of plasma

494   amino and fatty acids for four different glucose levels. The subplots A, B, C & D represents the

495   flux variations for plasma glucose concentration of 3mM, 5 mM, 10 mM and 15 mM,

496   respectively.At normal glucose levels, fatty acid synthesis is higher at low fatty acid and

497   moderately higher amino acid levels. It increases with increasing glucose and moderately high

498   levels of amino acids. It is inhibited at high fatty acid and high amino acid zone.
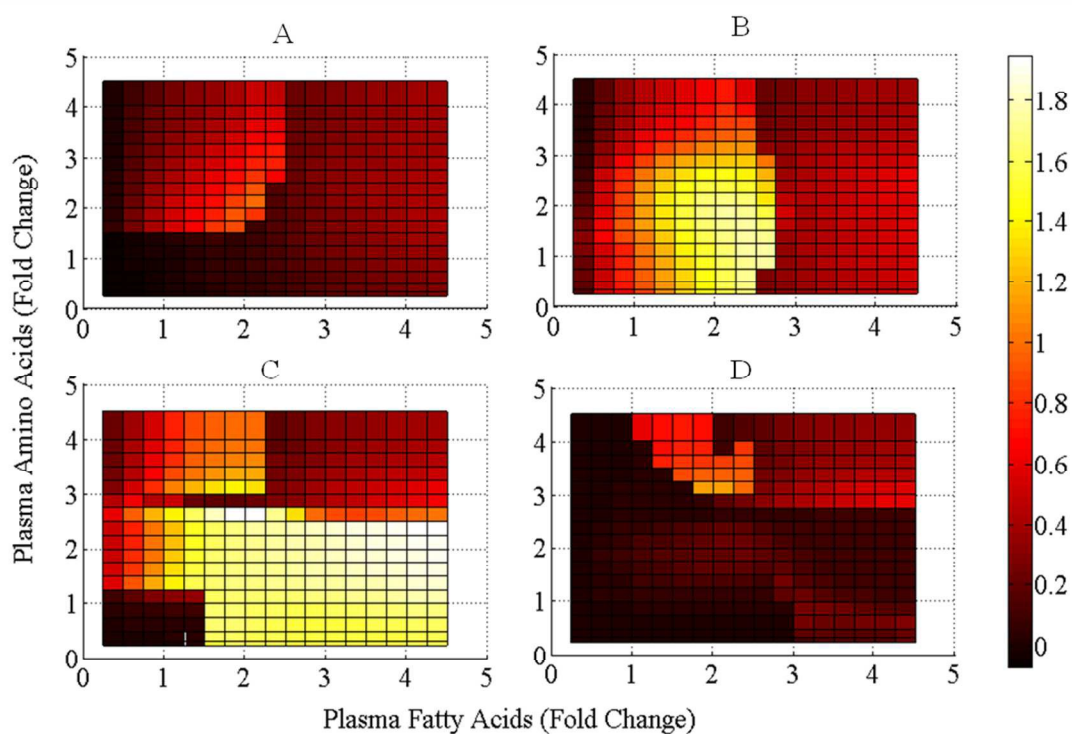
499

500   **Figure 16** Theflux ratio of triglyceride synthesis to triglyceride breakdown for varying levels of

501   plasma amino and fatty acids for four different glucose levels. The value below one represents

502   the net flux is towards triglyceride breakdown and vice versa.The subplots A, B, C & D

503   represents the flux variations for plasma glucose concentration of 3mM, 5 mM, 10 mM and 15

504   mM, respectively.Triglyceride synthesis decreases with lower and very high glucose levels and

505   increasing fatty acid levels under normal glucose levels. It is higher at moderate glucose, amino

506   acid and high fatty acid levels. However at very high glucose levels, higher amino acid level and

507   moderate fatty acid level increases TG synthesis.

508   **Cholesterol Metabolism**

509   The cholesterol biosynthesis flux is characterized by the flux through the HMGCoA(3-hydroxy-

510   3-methyl-glutaryl-CoA)reductase that catalyzed the conversion of HMGCoA to Mevalonate (a

511   rate limiting step in cholesterol biosynthesis pathway) (See Fig.17). Under low glucose levels the

512   cholesterol biosynthesis is the lowest and a marginal increase under normal glucose, fatty acid

513   and amino acid levels. The activation of glucagon under these conditions results in activation of

514   PKA which inhibits cholesterol synthesis. On further increasing glucose levels the cholesterol

515   biosynthesis increases further under marginally higher levels of amino acids and fatty acids.

516   Under very high plasma glucose levels, moderately high amino acids and the high fatty acid level

517   results in maximum flux towards cholesterol biosynthesis. This is due to the higher SREBP

518   levels activated by insulin and fatty acids under this condition. However, higher amino acid

519   levels reduce the flux towards the biosynthesis of cholesterol. SREBP a regulator of HMGR is

520   reduced due to inhibition of AKT at higher amino and fat acid levels, whereas fat activates

521   SREBP along with insulin, hence higher cholesterol synthesis (See S1 file Fig.S10).

522   **Amino Acid and Protein Metabolism**

523   The analysis shows that the amino acid uptake increases with increasing amino acid and fatty

524   acid levels, while it decreases with increasing glucose levels (See S1 file Fig.M9). This suggests

525   that the gluconeogenesis from amino acids is mainly operational under low glucose level.

526   Further, it can be noted that amino acid uptake is lowest under high glucose, low amino acids

527   and high fatty acid levels (See Fig. M9(C&D)). Higher glucose levels essentially reduce

528   gluconeogenesis which makes the amino acid uptake flux redundant. Since, amino

529   acidsaremainly a source of carbon for glucose and protein synthesis in liver, such a flux is

530   observed. It is also interesting to note that the conditions that show higher amino acid uptake

531   overlap with that of higher gluconeogenesis, indicating that amino acids are one of the major

532   substrates for gluconeogenesis. The protein metabolism was characterized by plotting the

533   normalized flux difference between protein breakdown and synthesis flux (See Fig.18). The

534   protein synthesis in liver is mainly under high amino acid and low fat levels.

535
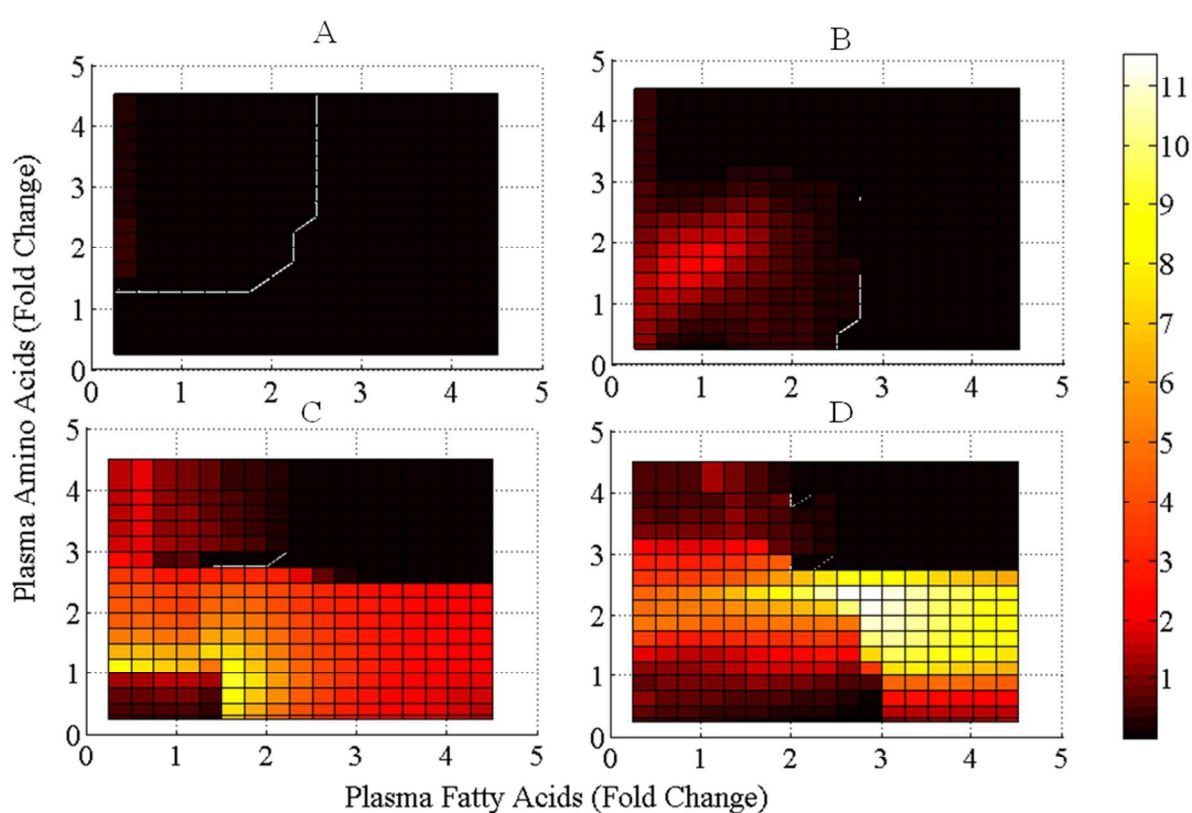
Figure 17 The cholesterol biosynthesis flux, that is represented by the flux trough HMGCoA

537   reductase flux which catalyzed HMGCoA to Mevelonate for varying levels of plasma amino and

538   fatty acids for four different glucose levels. The subplots A, B, C & D represents the flux

539   variations for plasma glucose concentration of 3mM, 5 mM, 10 mM and 15 mM, respectively.

540   Cholesterol synthesis increases with increasing amino acids to moderate levels while glucose is

541   maintained at normal levels. It increases with increasing glucose and fatty acid levels at higher

542   glucose concentration; however it decreases at higher amino acid levels. It is reduced at lower

543   glucose levels and inhibited at high amino and fatty acid levels.

544   Further, protein synthesis increases with higher glucose levels. However it is reduced with

545   increasing fatty acid levels, thereby increasing its breakdown under low glucose, low amino acid

546   and high fatty acid levels. Protein synthesis decreases with increasing fatty acids due to

547   inhibition of AKT and subsequent activation of PKA that activates protein breakdown. Wherein

548   the protein synthesis is regulated by insulin and amino acid mediated activation of mTOR and

549   S6Kp which also increases with increasing amino acid and glucose levels (See S1 file Figs.N11

550   and N12). It should be noted that, under low and normal plasma glucose levels, the protein

551   synthesis is in parallel to amino acids being channeled towards gluconeogenesis, whereas, under

552   high glucose levels, protein synthesis is in contrast to region of gluconeogenesis.

553   The balance of the nitrogen in the system is regulated through urea cycle(50),(51). The flux

554   through urea cycle is characterized by carbamoyl phosphate synthase flux that catalyzed

555   ammonia to carbamoyl phosphate (See Fig.19). The flux through urea cycle increases with

556   increase in amino acid levels and decrease in glucose and fatty acids levels in plasma. It can be

557   noted that under high protein and high glucose levels, moderately higher levels of fatty acid are

558   required to maintain the flux through urea cycle. Subsequently, it can be seen that ammonia

559   release is maximum under high fatty acid/ high amino levels wherein the urea cycle flux is

560   inhibited(See S1 file Fig. M10). This is due to the inhibition of the urea cycle flux due to the

561   activation of PPARα by fatty acids and deactivation of PKA due to increased glucose levels.

562   Thus, the ammonia in the system is also dependent on the dietary composition of fatty acids and

563   amino acids.

564
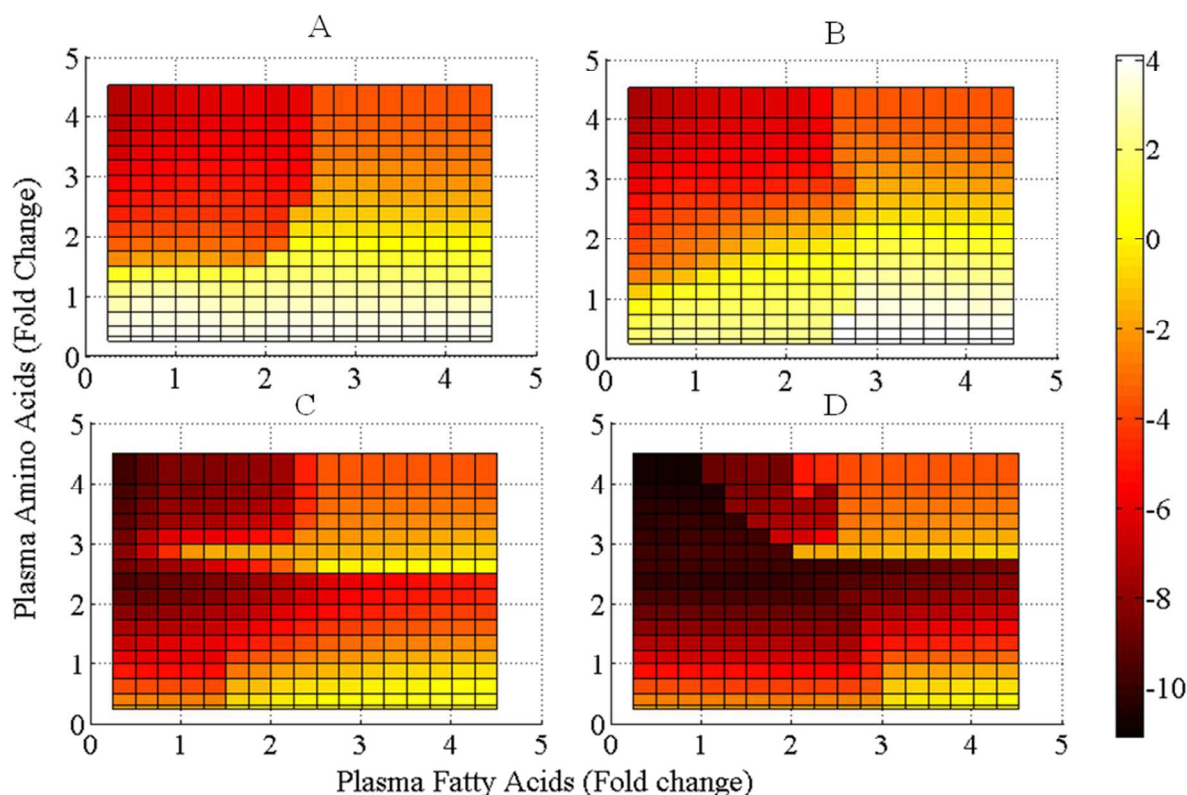
565

566   **Figure 18** Thenormalized flux difference between protein breakdown and protein synthesis for

567   varying levels of plasma amino and fatty acids for four different glucose levels. The negative

568   value on the color bar represents the net protein synthesis flux.The subplots A, B, C & D

569   represents the flux variations for plasma glucose concentration of 3mM, 5 mM, 10 mM and 15

570   mM, respectively.Protein synthesis increases with increasing amino acids and increasing glucose

571   levels and low fatty acid levels. However it is reduced by increasing fatty acid levels.
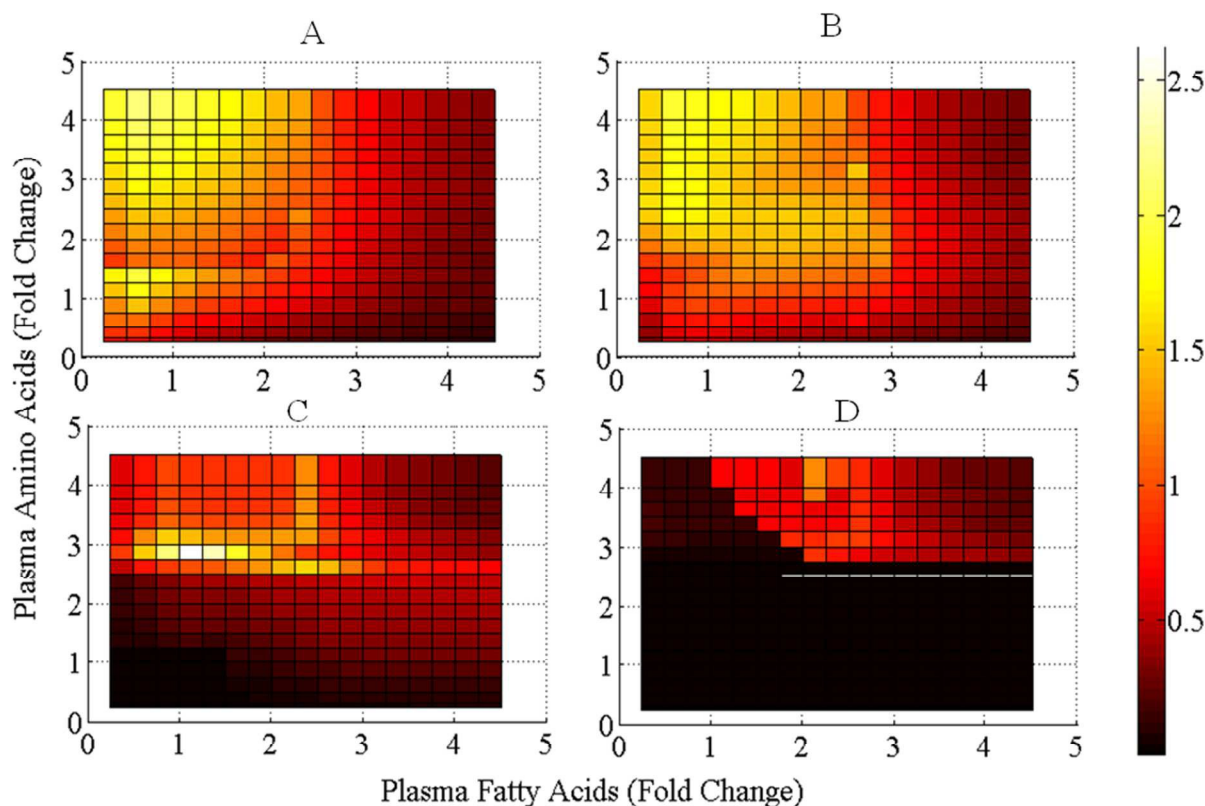
572

573 **Figure 19** The Urea cycle flux represented by the normalized rate of carbamoyl phosphate

574 synthase that catalyzed ammonia to carbamoyl phosphate for varying levels of plasma amino and

575 fatty acids for four different glucose levels. The subplots A, B, C & D represents the flux

576 variations for plasma glucose concentration of 3mM, 5 mM, 10 mM and 15 mM,

577 respectively.Urea cycle flux increases with increasing amino acids and decreases with increasing

578 glucose and fatty acid levels. However, under high amino acid and high glucose levels,

579 moderately higher levels of fatty acids restore the normal urea cycle flux. It is highest at low

580 glucose, low fat and high amino acid levels.

581

582 **Discussion**

583 In order to quantify the effect of plasma macronutrients on metabolic fluxes in liver, a detailed

584 model including signaling and transcriptional regulations was developed. The model predictions

585 revealed several signatures of metabolic performance under different levels of fat, amino acids

586 and glucose in the plasma. Using the regulatory signatures we could qualitatively rationalize

587 several experimental observations in the metabolic phenotypes associated disease states reported

588 in literature.The model reveals that glucose, fatty acids and amino acids have differential effects

589 on the secretion and activity of the metabolic hormones (insulin and glucagon) thereby

590 resultingin a highly nonlinear metabolic control. The analysis indicated that a steady state

591 metabolic flux is collectively determined by the regulatory effects of signaling components,

592 transcriptional factors and the metabolic controllers (ATP/ADP and NADH/NAD ratios).

593 Alternative to the results reported above, we summarize the overall effect of diet (plasma

594 macronutrient levels) on the key metabolic pathways in a tabular form (See supplementary file,

595 Excel file, S2_Table). The table reports a relative flux ratio to the flux under physiological

596 resting. The trends in the results of our model were motivated to explain the qualitative

597 metabolic responses observed in experiments reported in literature. However, the quantitative

598 validation of the model predictions with each of the experimental observations is out of the scope

599 of present manuscript.

600 *How high levels of fatty acids and proteins can increase gluconeogenesis and decrease*

601 *glycogen synthesis leading to hyperglycemia?*

602 The gluconeogenesis is known to be fairly constant in healthy individuals under varying dietary

603 perturbations (52). However, for steady state perturbations, the analysisdemonstrated that

604 gluconeogenesis was activated at lower plasma glucose levels andwas also induced even at

605   constant glucose levels with increasing fatty acid composition. These results were in agreement

606   with the observations reported on humans(1,3). This was due to the inhibition of insulin

607   signaling pathway that reduced the glycolytic flux and glycogen synthesis, resulting in a higher

608   net gluconeogenic flux. Moreover, under high plasma glucose levels with increasing amino acid

609   levels above 2.5 to 3 fold have shown to inhibit insulin action leading to de novo glucose

610   synthesis from amino acids. Similar effects were observed in the investigation on rats fed on

611   high protein diet(53). Chevalier et al. have observed such effects in obese individuals, wherein

612   increased rate of protein catabolism contributed to greater rate of gluconeogenesis and

613   subsequent increase in glucose release(16). The sensitivity of gluconeogenesis increased with

614   amino acids under higher glucose levels and similar results were also reported for a protein rich-

615   low carbohydrate diet in humans (54). The inhibition of insulin signaling pathway was associated

616   with enhanced effect of glucagon signaling pathway being responsible for glycogen breakdown

617   and gluconeogenesis, which represented an insulin resistant state.

618   Glycogen synthesis is a key mechanism in storing the excess glucose from the blood into liver.

619   Defects in glycogen metabolism have been shown to be one of the main reasons for

620   hyperglycemia(55,56). The glycogen synthesis flux was quite sensitive to plasma levels of amino

621   acids and fatty acids. Glycogen synthesis followed the plasma glucose and insulin levels,

622   whereas its potential was reduced at very high amino acid levels thereby disabling sufficient

623   glucose uptake. Such an effect of high protein diets on hepatic glycogen metabolism in mice and

624   rat have been documented in literature(10,57). Taylor et al have demonstrated that postprandial

625   glycogen storage flux follows the insulin to glucagon ratio in blood (58) which is in agreement

626   with our analysis. Under low glucose level (i.e. under starvation or higher physical activity),

627   where glycogen breakdown is anticipated, increasing amino acids can further increase glycogen

628   breakdown, whereas higher levels of fatty acids reduced glycogen breakdown. This reduction in

629 glycogen breakdown flux under high fat diet was also confirmed in rats (12,59). This suggested

630 that for an obese individual, whose circulating fatty acid levels are high, it would be difficult to

631 obtain a faster rate of glycogen breakdown and subsequent glucose release as compared to a

632 normal individual under lower plasma glucose condition.

633 *How high fat diets induce defects in TCA flux leading to an insulin resistance state?*

634 The TCA cycle in liver acts as an amphibolic pathway, which serves both anabolic and catabolic

635 purpose in hepatocyte through its ability of anaplerosis and cataplerosis, respectively (60). Under

636 surplus energy (ATP) condition the flux was diverted towards lipogenesis or amino acid

637 synthesis (anabolic) and under lower ATP states, the pyruvate, fatty acids and the amino acids

638 are collectively utilized for the synthesis of ATP (catabolic) and gluconeogenic precursors, via

639 TCA cycle. Therefore, the net abundance of these metabolites and the energy status of the cell

640 decidedwhether the TCA cycle operate under catabolic or anabolic mode. The analysis indicated

641 that the pyruvate dehydrogenase flux increased linearly with increasing glucose and decreased

642 with increasing fatty acid levels. However, under low glucose levels this flux increases with

643 increasing amino acid levels to cope up with the ATP requirement of the cell in a catabolic

644 manner. With increasing plasma glucose levels, excess glucose was diverted to lipogenesis via

645 pyruvate dehydrogenase that deployed partial TCA cycle in an anabolic manner. However, under

646 very high fatty acid levels, β-oxidation was activated due to another homeostatic constraint,i.e. to

647 maintain fatty acid levels. The pyruvate carboxylase flux increased under very high glucose and

648 high fatty acid levels, thereby diverting the TCA flux towards gluconeogenesis. Under higher

649 fatty acid levels PPARα was activated by PGC1 (PPAR gamma coactivator 1) mediated

650 mechanism which further enhanced fatty acid breakdown. Therefore, higher levels of Acetyl

651 CoA generated through β-oxidation inhibited pyruvate dehydrogenase thereby reducing the

652 glycolytic flux towards TCA cycle. TCA cycle was thus activated catabolically to utilize excess

653 Acetyl CoA in the form of energy or de-novo glucose synthesis. At cellular level, this

654 mechanism acts to economize the energy production through either of the substrates (glucose or

655 fat) under surplus conditions. The two observations of increased lipolysis and gluconeogenesis

656 were also confirmed by a study on humans reported by (11) and(14). Therefore, glucose

657 homeostasis is destabilized by excess fatty acids due to the inherent metabolic control in TCA

658 cycle which would eventually lead to a diabetic state, under high fat dietary intake.

659 *How lipogenesis and triglyceride synthesis are affecteddue to high carbohydrate and fat diet*

660 *leading to a diabetic state?*

661 In lipogenesis, fatty acid synthesis was favored with increasing glucose (up to 2 folds) levels and

662 moderate amino acid levels, however, it decreased with increasing fatty acid levels and very high

663 amino acid levels due to the inhibition of insulin signaling and activation of PKA (i.e. catabolic

664 activity). This suggested that lipogenesis was favored under low fatty acid and high glucose

665 levels which also assured the maintenance of fatty acid homeostasis in the cell. The variation in

666 lipogenic flux was in line with recent experimental studies performed on rats that were fed on

667 high carbohydrate and high fat diet (8,61). At very high glucose and fatty acid levels, the

668 lipogenic flux reduced due to the fall in ATP levels and inducedβ oxidation through the

669 activation of PPARα. One of the major fates of high levels of circulating plasma glucose was to

670 be stored as triglycerides via lipogenesis which also required higher consumption of ATP in the

671 cell. However, at higher glucose levels, oxidative phosphorylation was compromised due to high

672 insulin levels which inhibited the activators (PKA and calcium) of oxidative phosphorylation.

673 This puts forth a constraint on the disposal of glucose through lipogenesis at very high glucose

674 levels. Moreover, it was also limited by the correspondingly lower flux through the pentose

675　phosphate pathway which supplied NADPH (nicotinamide adenine dinucleotide phosphate) for

676　reducing power required for lipid synthesis. This phenomenon provided an insight into the patho-

677　physiology of diabetic conditions wherein higher plasma glucose might put a positive feedback

678　on its circulating levels due to reduction in the lipogenesis.

679　Similarly in triglyceride metabolism, triglyceride synthesis increased with increasing glucose and

680　fatty acid levels, however at very high glucose and amino acid levels the TG synthesis reduced.

681　The reduction in TG synthesis with increasing amino acid levels wasin line with the study that

682　demonstrated the reversal hepatic steatosis with high protein diet in mice (4,62,63). On the other

683　hand, triglyceride breakdown increased with decrease in glucose and fatty acid levels below the

684　normal level. This is also confirmed by (61) and (65) in their study on rats. Triglyceride

685　breakdown was further induced at very high glucose levels due to lack of ATP in the system. In

686　terms of diabetic pathogenesis, this suggested that, at very high glucose levels (>14mmol/l), fatty

687　acid levels might increase due to TG breakdown, which would further increase the negative

688　feedback of the fatty acid on the insulin action that aggravates the diabetic state by decreasing

689　the rate of glucose uptake.

690　***How a high carbohydrate diet increases cholesterol levels? How a high protein-low fat diet***

691　***can reduce cholesterol synthesis and help in reducinghypercholesterolemia?***

692　Liver is the major site for biosynthesis of Cholesterol.Cholesterol synthesis increased with

693　increasing glucose and fatty acid levels and reduced at very high amino acid levels. However it

694　increased with low fat and moderate amino acid levels under high glucose levels. These results

695　are in agreement with the dietary studieson humans and rats(66).This suggested that certain

696　amount of amino acid(1.25 to 2.5 fold of normal) was essential for cholesterol synthesis along

697　with fatty acid and glucose. Therefore, the analysis demonstratedthat maintainingthe plasma

698   amino acids either below 1.25 folds or above 3 fold (unusually high) levels can help in reducing

699   cholesterol even under higher glucose and fatty acid levels. These effect of low carbohydrate,

700   high fat and high protein diet on cholesterol homeostasis in mice was also documented (67). The

701   observation suggested that, higher levels of plasma amino acids under a diabetic state can help in

702   reducing the HMGCoA reductase fluxthere by reducing hypercholesterolemia.

703   *How high glucose and fat reduces protein synthesis? How a high fat diet increases plasma*

704   *ammonia levels?*

705   In case of protein metabolism, protein synthesis increased with increasing amino acids and

706   glucose levels and decreasing fatty acid levels. Protein breakdown increased with increasing

707   fatty acid levels and decreasing glucose and amino acid levels. These effects were also

708   demonstrated in rats fed on high fat diet (68,63). This is due to the inhibition of insulin signaling

709   and subsequent activation of glucagon signaling by higher fatty acid levels. The metabolic flux

710   observed under high fat levels explained the limitation of protein synthesis or decrease in muscle

711   density under diabetic state. Although higher glucose levels help in protein synthesis, when

712   followed by higher fatty acid levels the protein synthesis was hampered. The urea cycle

713   facilitated the homeostasis of the ammonia that is generated during amino acid breakdown. The

714   urea cycle flux increased with higher amino acid and lower glucose levels under moderate fatty

715   acid levels(69). The higher amount of amino acid influx to the liver induced a gluconeogenic

716   state in liver; wherein most of the amino acids were used for de novo synthesis of glucose.

717   Therefore, the nitrogen part of the carbon backbone of the amino acids was liberated as ammonia

718   which was disposed through urea cycle(70). With increasing glucose levels the potential of urea

719   cycle decreased due to reduction in gluconeogenic flux by insulin and utilization of amino acids

720   for protein synthesis. Moreover, with increasing fatty acid levels, the levels of ammonia rose

721 with increasing amino acids due to reduction in the urea cycle flux. A recent study demonstrate

722 the suppression of urea cycle enzymes by a high fat diet in hamsters (7).Due to its neurotoxicity

723 the ammonia levels were strictly under homeostatic control, therefore even 2 to 3 fold increments

724 in plasma ammonia levels are detrimental. Hence, the analysis indicated the importance of not

725 allowing the circulating levels of plasma fatty acid and amino acid levels to go very high

726 simultaneously for ammonia homeostasis.

727 *How high protein and fat levels can affect hepatic glucose release leading to hypoglycemic or*

728 *hyperglycemic states?*

729 One of the important transport flux is the hepatic glucose release which is reported to be

730 distorted in case of diabetic condition(71). Insulin is known to regulate hepatic glucose

731 production in direct and indirect mechanisms (72). The analysis demonstrated that at lower

732 plasma glucose and with increasing plasma amino acid levels the hepatic glucose release rate

733 increased as reported by (73), whereas at high amino acid and fatty acid levels the release rate

734 was restricted to a normal level (instead of increasing).Under conditions of starvation or higher

735 physical activity, the lower plasma glucose levels led to an increase in the plasma glucagon

736 levels. Glucagon triggers gluconeogenesis and glycogenolysis with the activation of cAMP, PKA

737 and calcium signaling in liver. However at very high levels of amino acids and fatty acid levels

738 insulin secretion was triggered which further inhibited the action of PKA through AKT. Under

739 such a condition, although the plasma glucagon level was high there was no subsequent rise in

740 the hepatic glucose release. This shows that higher circulating levels of plasma amino and fatty

741 acids can reduce hepatic glucose release irrespective of the plasma glucagon levels.

742 Under resting state and normal glucose levels, increasing fatty acids to 3-4 folds increased

743 glucose release by 20-25% due to the inhibition of AKT by fatty acids. These effects of high fat

744   diet on fasting glucose were demonstrated in healthy men (74). Under the postprandial state, with

745   increasing plasma glucose levels, the glucose uptake increased;however, the uptake rate

746   decreased with increasing amino acid and fatty acid levels, even leading to glucose release. This

747   reduction in insulin's action under high fat and relatively low carbohydrate diet is demonstrated

748   in a study conducted on humans (75). Under such condition, the higher levels of amino acids

749   triggered glucagon secretion and subsequent activation of PKA and S6K which inhibited insulin

750   signaling along with further inhibition by fatty acid.Henkel et al. have reported a similar

751   increment in plasma glucagon levels under postprandial state in the subjects with glucose

752   intolerance and Type 2 diabetes(76). Moreover, it led to a lower ATP/ADP ratio which limited

753   the conversion of glucose to G6p leading to higher cellular glucose and the reversal of glucose

754   uptake flux. Therefore, even under high levels of circulating plasma insulin, the cellular state

755   was shifted to a catabolic mode with activation of gluconeogenesis instead of glycolysis and

756   resulted in glucose release instead of its uptake. Such a condition depicted a diabetic state or

757   insulin resistance irrespective of the insulin levels just due to the metabolic shift that the

758   macronutrients induced in the cells(15).In a diabetic state, wherein plasma glucose levels are

759   already higher, higher intake of amino acids and fatty acids can further aggravate glucose levels.

760   ***How high glucose levels can affect hepatic fatty acid uptake leading to dyslipidemia and non-***

761   ***alcoholic fatty liver disease (NAFLD)?***

762   Similarly, higher levels of plasma fatty acids and triglycerides are also indicators of a disease

763   state in obesity and dyslipidemia(77,78,79). The hepatic fatty acid uptake increased with 2-2.5

764   fold of plasma fatty acid levels and was further reduced at higher fatty acid levels under resting

765   glucose condition; however, it increased with 2-2.5 fold increase in plasma glucose levels. The

766   fatty acid uptake was mainly dependent on the cellular ATP/ADP ratio and insulin levels. The

767   fatty acid uptake was drastically reduced at very high glucose levels except for very high levels

768   of plasma amino acids and fatty acids. This was due to the lower levels of ATP under very high

769   glucose levels which limited the conversion of fatty acids to triglycerides. In such a condition,

770   even though the plasma insulin levels were higher the hepatic fatty acid uptake was reduced

771   which can lead to higher levels of plasma fatty acids due to distortion in the capacity of this flux

772   to maintain homeostasis(3,80).

773   The triglyceride release followed the fatty acid uptake flux in the range of lower to moderate

774   levels of plasma glucose levels; however, it was inhibited at higher levels of amino acids due to

775   inhibition of insulin signaling. The release was completely suppressed at very high glucose levels

776   due to lack of cellular ATP levels and insulin resistance induced by very high amino acid and

777   fatty acid levels(81). Although fatty acid uptake increased under very high levels of all the three

778   macronutrients, thetriglyceride synthesis was suppressed. This condition can result in higher

779   levels of cellular fatty acid and further inhibition of insulin signaling by a DAG-PKC mediated

780   mechanism thereby leading to Insulin resistance(82), and non-alcoholic fatty liver disorder(80,82,

781   83). The above observation provided insights into how a diabetic state (hyperglycemia) can lead

782   to higher plasma fatty acid levels and the resulting metabolic states can put a positive feedback

783   on insulin resistance, and thus stabilizing the diabetic state.

784   **Conclusion**

785   In summary, the metabolic status of a tissue depends upon the ratios of the metabolic controllers

786   such as ATP/ADP and NADP/NADPH, and the phosphorylation states of the regulatory

787   signaling proteins. The metabolic state of a tissue then influences the transport fluxes from the

788   tissue which in turn govern the plasma metabolite levels. The transport fluxes are the resultant

789   effects of plasma macronutrient levels and the subsequent hepatic metabolic state. The

790　　phosphorylation states of the signaling molecules also strongly influence the levels of ATP/ADP

791　　ratio. This is further translated to overall metabolic pathways that use ATP-ADP as co-substrates

792　　and affects the synthesis and transport process of key metabolites. In this study, we demonstrated

793　　the perturbations in these regulatory mechanisms due to plasma macronutrients and several

794　　resulting metabolic states representing healthy and disease states.

795　　Thus, thedeveloped model provided insights on the functioning of cellular metabolism that arise

796　　due to several combinations of the plasma levels of the major macronutrients that are part of our

797　　daily diet. These plasma profiles are highly dynamic in nature due to time varying dietary

798　　interventions and cells have to constantly regulate its metabolism to achieve homeostasis. Any

799　　perturbations due to either external factors such as diet and exercise or internal factors such as

800　　hormonal ratios and signaling or transcriptional events can influence the metabolic phenotype.

801　　Therefore, our analysis reveals the signatures of plasma metabolite profiles that can defile the

802　　homeostasis due to de regulatory effects caused by specific levels of macronutrient and their

803　　combinations. The analysis can be further extrapolated to understand the dietary requirements so

804　　as to assist the homeostasis by appropriate dietary composition. Nevertheless, this study helps in

805　　visualizing the metabolic profiles under abnormal plasma levels of key metabolites which might

806　　occur due to various disease states.

807

808

809

810

811 **Methodology -Mathematical Model for Liver Metabolism**

812 The model consists of central metabolic pathway including glycolysis, gluconeogenesis,

813 glycogen metabolism, TCA cycle, fatty acid synthesis and oxidation, protein synthesis and

814 breakdown, urea cycle, pentose phosphate pathway, cholesterol biosynthesis and hexoseamine

815 pathway(See Fig 2)(34,35,38,42,55,84). The model was further integrated with sub-models for

816 several signaling and transcription networks. Moreover, we have extended the model to

817 incorporate the whole body plasma metabolite homeostasis to analyze its effect on liver. The

818 developed model integrates several reported sub-models in conjunction with models developed

819 for signaling and transcriptional regulation adopting a systems level approach (83). The overall

820 model for the liver metabolic module consisted of 272 rate equations, 170 ODEs and 801

821 parameters.The integrated model is composed of four modules viz., (1) Blood (metabolites and

822 hormones), (2) Metabolism, (3) Signaling and (4) Transcription. The detailed model and

823 parameters are explained in supplementary file S3.

824 The blood module represents the dynamics of plasma metabolite concentrations at whole body

825 level. It includes the kinetics of hormonal secretions (i.e. insulin and glucagon) in the blood from

826 pancreas in response to plasma macronutrient levels(86–88). The blood module accounts for the

827 facilitated transport from blood to tissue of seven metabolites viz., glucose, lactate, pyruvate,

828 amino acids, fatty acids, glycerol, triglycerides, and the passive transport of oxygen and carbon

829 dioxide(84).

830 In the metabolism module, the metabolic pathways (as mentioned above) required for the

831 processing carbohydrates, lipids and proteins in liver were modeled along with their regulations

832 at metabolic, signaling and transcriptional levels.The hormonal (insulin and glucagon) and

833 nutrient (glucose, amino acids and fatty acid) signaling pathways were adopted from literature

834   (43,44,89) and integrated together for metabolic regulation. The signaling network composed of

835   the feedbacks and crosstalk between insulin signaling mediated through AKT and mTOR

836   signaling and glucagon signaling mediated through calcium and cAMP signaling. Furthermore,

837   the transcriptional network was modeled to incorporate the long-term/ genetic effects of plasma

838   macronutrients on the synthesis and activation of metabolic enzymes and the signaling proteins.

839   The transcriptional network consisted of the ten transcriptional factors such as

840   SREBP,ChREBP,CREB (cAMP response element-bindingprotein), CEBPα (CCAAT enhancer

841   binding protein alpha),PGC1, TRB3, FOXO,PPAR (γ,α,β) andAMPK along with the inputs from

842   the signaling and metabolic networks.

843   The regulation of a metabolic enzyme by a signaling/ transcriptional component was modeled by

844   assuming the parallel activation of other enzymes in a linear pathway(90). This assumption

845   ensures that the activation or inhibitions of all the enzymes in a linear pathway are similar to

846   yield a balanced flux through the pathway. The regulatory effects of the signaling endpoints were

847   incorporated in the metabolic reactions, wherein, these regulations were assumed to influence the

848   maximal rate of an enzymatic reaction. The anabolic regulatory effects on the metabolic

849   pathways were mediated by the insulin signaling components and the catabolic effects were

850   mediated by the glucagon signaling components.The modules are interconnected through several

851   common components such as metabolites and active hormonal concentrations that synchronize

852   together to establish a metabolic state as a result of an input function. The parameters of the

853   models were obtained by flux balance analysis, regression and by the least square fit technique

854   used for in-silico fitting of an expected output response for a sub network. The optimal estimates

855   of the parameters were those that gave best least square fit by minimization of the sum of errors

856   for an objective function to the data obtained from literature either through experimental data or

857   through validated model simulations. We tried to retain the reported parameter values from the

858   source models allowing minimal deviation in them. We only tended to estimate the parameters

859   for integrating the sub modules. Each sub module was independently calibrated to a

860   known/reported experimental profiles and then integrated together to minimize the sum of the

861   errors after integration. This allows us to constrain our calibration space and minimize the risk of

862   overfitting. In this sense we reduce the degree of freedom by relying more on the reported

863   parameters and models and the experimental data to fit the modular parameters (interactions and

864   crosstalk between modules).

865   **Blood Module**

866   The blood module depicts the surrounding medium of the liver tissue. It consists of the

867   metabolites that have been considered as transport metabolites to the tissues and the hormones

868   that are responsible for the metabolic regulations in the tissue. Two pools of the blood streams

869   were considered viz., arterial blood and capillary blood (i.e. equivalent to venous blood) supplies

870   to the tissue. It was assumed that the arterio-venous difference in the metabolite concentration is

871   equal to the tissue metabolite uptake. Therefore the events of plasma metabolite flow was

872   considered such as, the arterial blood is supplied to the capillary bed around the tissue and the

873   plasma metabolites diffuse either passively or by facilitated manner to the interstitial fluid

874   surrounding the tissue membrane from where the metabolites are taken up by the tissue. The

875   interstitial fluid and capillary plasma metabolite concentrations are assumed to be in equilibrium.

876   The resultant blood after the exchange and transport of the metabolites is termed as the venous

877   blood. The physiological blood flow rate and the volume of the blood were considered to be

878   constant. As per the experimental evidence, the blood flow rate regulation by the plasma

879   hormonal concentrations (insulin) was also accounted.

880   We have also considered the plasma concentrations of two major metabolic regulatory hormones

881   namely, insulin and glucagon. The secretion of hormones is known to be regulated by nutrients

882   in the plasma(19,91).The plasma concentrations of insulin were modeled as a function of plasma

883   glucose, amino acids and fatty acids by fitting an appropriate Hill function to the experimental

884   data from literature(24–27,92).The Hill fit for the plasma insulin levels with respect to plasma

885   glucose was obtained from experimental data reported by Konig et al. 2012.

886   The experimental data for the effect of amino acids on plasma insulin was extracted from the

887   dynamical data reported by Calbet and Maclean, 2002 and Loon et al. 2000, for different amino

888   acid inputs(86,88)The data for the effect of fatty acids/lipids on plasma insulin was extracted

889   from the dynamical data reported by Gravena et al. 2002 and Manco et al. 2004(93,94) Since

890   there was scarcity of the dose response curves for amino acid and fatty acid effects on plasma

891   insulin levels, the dynamical data was used to obtain steady state points and was used to obtain

892   the Hill fits based on the fold changes in plasma insulin levels for different amino acids (See S1

893   file Figure M1 (A,B,C).

894   The plasma glucagon concentration was modeled as function of plasma glucose and amino acid

895   concentrations (95,96). In our study, we varied the arterial plasma concentrations of glucose,

896   amino acids and fatty acids and measured the steady state response of the metabolic fluxes and

897   the metabolite concentrations(86–88,97).

898   The rate of insulin secretion was modeled as

899    $$Ins_{Sec} = \left(V_{Glu} * \frac{Ca_{Glu}{}^{ng}}{Ca_{Glu}{}^{ng} + K_{Glu}{}^{ng}} \right) + \left(V_{AA} * \frac{Ca_{AA}{}^{na}}{Ca_{AA}{}^{na} + K_{AA}{}^{na}} \right) + \left(V_{FFA} * \frac{Ca_{FFA}{}^{nf}}{Ca_{FFA}{}^{nf} + K_{FFA}{}^{nf}} \right)(1)$$

900   WhereV_{Glu}, $V_{AA}$and$V_{FFA}$are the maximal insulin concentrations with respect to glucose, amino

901   acids and fatty acids, respectively. Ca_{Glu}, $Ca_{AA}$and$Ca_{FFA}$are the concentrations of glucose, amino

902 acids and fatty acids in the arterial blood. ng, ng, nf and K_{Glu}, K_{AA}, K_{FFA} are the hill coefficients and

903 the half saturation constants for glucose, amino acids and fatty acids, respectively. This rate was

904 further incorporated into the kinetic model for the liver and plasma insulin levels developed by

905 Dalla Mann et.al. (2007) The plasma glucagon concentration was modeled as function of glucose

906 and amino acid levels(86,97,98).

907 $$Glcn_{Sec} = \left(\frac{V\_Glu_{Glcn}}{1+\left(q1*exp(p1*(Ca_{Glu}-Ca_{Glub}))\right)}\right) + V\_AA_{Glcn} * \left(\frac{Ca_{AA}^n}{Ca_{AA}^n+K_{AA}^n}\right)(2)$$

908 Where V_Glu_{Glcn} is the maximum glucagon infusion rate, $q1$ and $p1$ are the weight factor and the

909 rate, respectively. V_AA_{Glcn} is the maximum infusion rate of glucagon due to amino acids and n and

910 K_{AA} are the corresponding Hill coefficient and half saturation constant. To obtain the plasma

911 concentrations of glucagon, these secretion rates were incorporated into the kinetic model

912 developed by Liu et.al. (2009).

913 The effect of plasma insulin concentration on the blood flow was derived by fitting a Hill

914 equation to the profiles from the literature. The effect of plasma insulin on hepatic blood flow

915 was modeled from the dynamical data reported by Fryan 2003(99), wherein the 2.5 fold change

916 in blood flow was reported for a 5 fold change in the plasma insulin levels (SeeS1 file Fig.M1

917 (D).

918 $$Ins_{bld_{Eff}} = 1 + \left(Vmax * \left(\frac{INS^n}{(INS^n)+(K_{Ins})^n}\right)\right)(3)$$

919 Where, $Vmax$ is the maximum rate, INS is the plasma insulin concentration, n is the Hill

920 coefficient and K_{Ins} is the MichaelisMenten constant. The passive and facilitated metabolite

921 transport across the tissue and blood compartment was modeled as per Eqn.5 and Eqn.6

922 respectively.

923 $$Tis_{tjpassive} = \epsilon_j * (C_{bj} - C_{cytj})(4)$$

924 $$Tis_{tjFaciltated} = T_j * \left(\frac{C_{bj}}{K_{bj}+C_{bj}} - \frac{C_{cytj}}{K_{cytj}+C_{cytj}}\right)(5)$$

925 Where, C_{bj} and C_{cytj} are the *j*th metabolite concentrations in the blood and the cytosol,

926 respectively.$\epsilon_j$andT_j are the effective permeability issue surface are product and the maximal

927 transport rate of the metabolite across the tissue for passive and facilitated transport,

928 respectively.K_{bj}andK_{cytj} are respective saturation constants for blood and cytosolic metabolites

929 for blood tissue transport.The metabolite concentrations in the blood were modeled using the

930 framework as given below.

931 $$\frac{dc_{bj}}{dt} = \left\{Bld_{flw} * Ins_{bld_{Eff}} * (C_{aj} - C_{bj}) - Tis_{tj}\right\}/(V_{bld})(6)$$

932 Where, $C_{bj}$is the *j*th metabolite concentration in the capillary blood, Bld_{flw} is the blood flow rate

933 to the liver, $Ins_{bldEff}$is the effect of the insulin on blood flow, C_{aj} is the *j*th metabolite

934 concentration in the arterial blood, Tis_{tj} is the rate of metabolite transport across the tissue and

935 blood, V_{bld} is the volume of the capillary blood.

936 **Metabolism Module**

937 This module consists of a detailed model of hepatic metabolism that comprises of the central

938 metabolic pathway including glycolysis and gluconeogenesis, glycogen synthesis and

939 breakdown, TCA cycle, oxidative phosphorylation, fatty acid synthesis and oxidation, protein

940 synthesis and breakdown, urea cycle, pentose phosphate pathway, cholesterol biosynthesis and

941 hexose amine pathway. The model for glycolysis, glycogen metabolism and gluconeogenesis

942 was adopted from Konig et al. 2012. The detailed model was developed for lipid and amino acid

943 and lipid metabolism which was further integrated with the existing model for carbohydrate

944 metabolism.The general form of metabolic reactions was written in Michaels Menten formalism.

945 $$\frac{dM_i}{dt} * V_c = \sum_{j=1}^{nj} V\_prod_j - \sum_{k=1}^{nk} V\_cons_k + Tis_t \quad (7)$$

946 Where M_i is the concentration of the ith metabolite, V_c is the volume of the compartment (cytosol

947 or mitochondria), V_prod_j and V_cons_k is the rate of production and consumption of the ith

948 metabolite, respectively.Tis_t is the transport rate of the metabolite across blood cytosol or cytosol

949 mitochondrial compartment. The production and consumption rates were modeled using the

950 MichaelisMenten functions as given below

951 $$V\_prod_j = V_{max_j} * Reg\_Vprod_j * \prod_{s=1}^{nsj} \left(\frac{M_{s,j}}{M_{s,j}+Km_{s,j}}\right) \quad (8)$$

952 $$Reg\_Vprod_j = \prod_{r=1}^{nrj} \left(Reg_{Act\,r,j} * Reg_{Deact\,r,j} * Reg_{pi} * Reg\_Sig\_trans_{r,j}\right) \quad (9)$$

953 $$Reg_{Act\,r,j} = \left(\frac{A}{A+K_j}\right) Reg_{Deact\,r,j} = \left(\frac{K_i}{I+K_i}\right) Reg_{pi} = \left(\frac{A}{A+Ki*\left(1+\frac{I}{Kp}\right)}\right) \quad (10)$$

$$Reg\_Sig\_trans_{r,j} = W_f * \left(1 + \sum_a^{an} Sig\_act_a + \sum_b^{bn} Trans\_act_b\right) * \prod_d^{dn} (Sig_{deact} * Trans_{deact})$$

954 Where V_{max_j} is the maximum rate of the jth reaction, Reg_Vprod_j is the product of the regulation

955 by the metabolite, signaling and the transcription.$M_{s,j}$ is the sth metabolite in the jth reaction and

956 $Km_{s,j}$ is the corresponding saturation constant. A and$I$ are the activators and the Inhibitors

957 pertaining to the activatory $(Reg_{Act\,r,j})$ or inhibitory $(Reg_{Deact\,r,j})$ regulation of the flux,

958 respectively. $Reg\_Sig\_trans_{r,j}$ is the regulation exerted by the signaling and transcriptional

959 networks, wherein Sig_act_a is the positive regulation by the ath signaling molecule and

960 $Trans\_act_b$ id the positive regulation by the bth transcription factor. Sig_{deact} and $Trans_{deact}$ are

961 the negative regulations exerted by the signaling and transcription events on the jth flux,

962 respectively.

963 **Modeling Metabolic Regulation**

964 The regulation of the signaling component on the metabolic enzymes were modeled by assuming

965 parallel activation mechanism wherein, if a signaling/transcription component is known to

966 regulate a enzyme in a certain manner (activation or inhibition), then the subsequent linear

967 pathway was assumed to be correspondingly activated by that signaling/transcription component

968 to ensure the flux balance. Apart from this, the regulations by several signaling/transcription

969 components on a single enzyme was assumed to be by the OR gate for activation effects and by

970 AND gate for inhibitory effects as given in Eq.17.The formalism used for modeling these

971 regulations are as given below.An example of glycolysis regulatory function is illustrated below.

972 $AKt_{Ptv_{glysis}} = V_{akt} * \left(\frac{AKT^n}{AKT^n + Km_{akt}{}^n} \right)(12)$

973 $SREBP_{Ptv_{glysis}} = V_{srebp} * \left(\frac{SREBP^n}{SREBP^n + Km_{srebp}{}^n} \right)(13)$

974 $CHREBp_{Ptv_{glysis}} = V_{chrebp} * \left(\frac{CHREBp^n}{CHREBp^n + Km_{chrebp}{}^n} \right)(14)$

$AMPK_{glysis} = V_{ampk} * \left(\frac{AMPK^n}{AMPK^n + Km_{ampk}{}^n} \right)(15)$

$FOXO_{Ntv} = \left(\frac{Km_{foxo}{}^n}{Km_{foxo}{}^n + FOXO^n} \right)(16)$

$Reg\_(Glu\_(G6p))$

$$= (0.25).* (1 + AKt\_(Ptv\_glysis) + SREBP\_(Ptv\_glysis) + AMPK\_(Eff\_glysis)$$
$$+ CHREBp\_(Ptv\_glysis)) * FOXO\_Ntv; \qquad (17)$$

975

976   The regulations of the metabolic reactions were modeled to modulate the metabolic enzymes.

977   Several signaling and transcription factors are known to regulate metabolism (See Table II). The

978   influence of various signaling and transcriptions such as activation and deactivation of these

979   enzymes were derived from the dose response data from the literature. The unknown rates were

980   deduced by the fitting the output curve to the desired response and followed by appropriate

981   parameterization. The unknown rates for the metabolic regulation by the signaling pathways

982   were obtained by fitting the pathway rate parameters to the time-course data of plasma

983   metabolite levels (i.e. glucose, amino acid and fatty acids). The rational was to obtain the fold

984   change in the metabolic rates required to obtain the reported experimental profiles for plasma

985   metabolite. These fold changes were translated to the appropriate Hill fits for the effect of

986   signaling endpoints on the metabolic enzymes. From these Hill fits the three parameters *Vmax,*

987   *Km* and *n* were deduced, wherein the '*Vmax*' is the maximum fold change required, '*Km*' the half

988   saturation constant and '*n*' as the Hill coefficients assumed to be sensitive(*n*=2-4).

989   We have included the pentose phosphate pathway, urea cycle, cholesterol biosynthesis(100) and

990   hexoseamine pathways (101)(102) along with the central metabolic pathway. While pentose

991   phosphate pathway is the major source of NADPH, urea cycle takes care of the deamination or

992   removal of the ammonia (NH4) generated while gluconeogenesis and amino acid catabolism,

993   through urea(51,69). Hexoseamine pathway is the indicator of the metabolic status of the cell

994   under nutrient stress. This pathway is composed of the inputs from the derivatives of glucose,

995   amino acids and the fatty acid metabolism. At higher levels of these metabolites, the

996   glucosamine formation are triggered which further is responsible for the glycosylation of the

997   metabolic enzymes. N-acetyl glucosamine an end product of the hexoseamine pathway is the

998   indicator of the metabolic stress in the cell.

999 **Table II** Regulation of hepatic metabolism by metabolites

Reaction Enzyme	Positive regulation	Negative regulation
Glucokinase		F6p
Phosphofructokinase	AMP	Citrate
Glycogen phosphorylase	AMP	Glucose
Ga3p dehydrogenase		Glucose
Pyruvate kinase	F16p	Amino Acids
Pyruvate dehydrogenase		NADH, Acoa (Pi)
Citrate synthase	AMP	
Isocitrate dehydrogenase		Scoa (Pi)
AKG dehydrogenase	AMP	Scoa (Pi)
Citarte shuttle (103)		Palcoa(Pi)
Cit_Acoa_OAA (ATP citrate lyase)		Palcoa(Pi)
Acoa_MalcoA (Acetyl CoA Carboxylase)		Palcoa(Pi)
FFA_Palcoa (Acyl CoA synthase) (Saggerson, 2008)		Malcoa (Pi)
Palcoa_Acoa (β oxidation)		Acoa (Pi)
Carnitine shuttle (Carnitine acyltransferase)		Malcoa
Gmt_AKG (Glutamate dehydrogenase)		FFA
Acoa_Gmt_NAG (N acetyl glutamate synthatase)	Arginine	
NH4_Crbphos (Carbomyl phosphate synthase)	NAG	
Citrulin_Arg (Argininosuccinate lyse)	AMP	
(Glucosamine 6 phosphate N acetyl transferase)	FFA	Glnac (Pi)

(N acetyl glucosamine pyrophosphorylase)	Glucose	
HMGcoa_Mevl (HMGCoA reductase)		Mevl(Pi)

1000

1001 **Signaling Module**

1002 This is for the first time in literature, that we have integrated the hormonal signaling (Insulin and

1003 Glucagon) pathway along with the calcium, cAMP and mTOR signaling pathways. These

1004 models were adopted different literature sources and integrated together with the appropriate

1005 modeling formalisms. The model for Insulin signaling was adopted from the Sedghat et al.

1006 (2002) and the Glucagon signaling was adopted from Mutalik et al.(44) and Xu et al(42). Insulin

1007 and glucagon hormones and the signaling pathways are mutually antagonistic pathways wherein

1008 the downstream of insulin signaling inhibits the activation of cAMP i.e. the glucagon signaling

1009 component. Similarly the calcium activated DAG increases the phosphorylation of inactivated

1010 PKC which further inhibits the insulin signaling through IRS. While AKT and GSK3 acts as

1011 major anabolic regulatory signaling component of insulin signaling pathways, cAMP and PKA

1012 are the major metabolic regulatory components of the glucagon signaling pathway. Further, AKT

1013 and amino acids signal to activate mTOR(104,105) and its downstream S6K that has an

1014 inhibition of IRS(21–23,89,106). Table III lists the feedback regulations in the signaling

1015 integrated pathways.The general formalism of modeling the signaling pathways is as given

1016 below

$$\frac{dS_i}{dt} = K_{synth} + \left(\sum_{j=1}^{nj} K_{phs_j} * S_i \right) * R_{preg_j} - \left(\sum_{k=1}^{nk} K_{dphs_k} * S_i \right) * R_{dpreg_j} - K_{deg} * S_i \quad (18)$$

1017   Where, K_{synth} and K_{deg} are the basal synthesis and degradation rate of ith signaling protein

1018 S, K_phs_j and K_dphs_k are the phosphorylation and the dephosphorylation rates of the signaling

1019   molecule, respectively. R_preg_j and R_dpreg_j are the   regulatory interactions of the

1020   phosphorylation and dephosphorylation of S, respectively.

1021   The regulatory effects of the signaling endpoints were incorporated in the metabolic reactions,

1022   wherein, these regulations were assumed to influence the maximal rate of an enzymatic reaction.

1023   The anabolic regulatory effects on the metabolic pathways were mediated by the insulin

1024   signaling components and the catabolic effects were mediated by the glucagon signaling

1025   components. The appropriate regulatory functions were modeled to integrate the signaling

1026   pathways to the metabolic pathways as described in the previous section.

1027   **Table III** Regulation of hepatic metabolism by Signaling components.

Signaling Components	Positive Regulation	Negative Regulation	References
IRS		PTP, PKC, S6K	(21)
AKT	mTORC2	Glnac, TRB3	(107)
PKC	DAG, Glnac, FFA		(28,29)
GSK3	PP1, Phk,	Cal, PKA, FFA	(108)
mTOR	Amino acids		(109)
S6K	Amino acids	AMPK	(110)
TSC	AMPK	AKT	(111,112)
cAMP	Gprt,	PDE3	(113,114)
PKA	cAMP		(115)
PDE3	AKT	PKA	(116)

1028

1029 **Transcriptional module**

1030 The metabolism in liver is known to be regulated by several transcription factors(117) such as

1031 SREBP(118),(119),(120)],ChREBP(121), PPAR (γ,α,β) (122),(123), CREB, CEBP (124), PGC1,

1032 TRB3, FOXO (125)and AMPK (126). Table IV lists the components that inter-regulate

1033 transcriptional factors. Although it is known that the glucose uptake by liver is mediated by

1034 GLUT2 which is known to be insulin independent, the expression of GLUT2 is regulated by the

1035 insulin dependent transcriptional factor SREBP 1c and Glucose. SREBP1c is activated in PI3K

1036 dependent manner and is responsible for the expression of Glucokinase enzyme, a rate limiting

1037 step in the glycolysis. Moreover, the expression of glycolytic and lipogenic genes are regulated

1038 by the action of SREBP1c, in the liver. Higher glucose levels also triggers the activation of a

1039 ChREBP transcription factor i.e. responsible for glucose mediated up regulation of lipogenesis

1040 through LPK, ACC and FAS gene transcription. Insulin signaling along with fatty acids activates

1041 a transcription factor PPARγ that is responsible for fatty acid transport and triglyceride synthesis

1042 in the liver. The catabolic transcriptions are mediated by the glucagon signaling, wherein cAMP

1043 activated PKA phosphorylates the transcription factor CREB which induces the transcription of

1044 the genes responsible for the enzymes of the gluconeogenesis pathway such as PEPCK, G6Pase

1045 and pyruvate carboxylase. CREB further activates the gluconeogenic cofactor PGC1 which

1046 increases the expression of the gluconeogenic genes. Another transcription factor activated under

1047 low glucose level and triggered by cAMP is CEBPa that regulates the transcription of the genes

1048 responsible for the ammonia metabolism i.e. urea cycle under higher protein diets or excessive

1049 amino acid breakdown during exercise. PPARα is the transcriptional activator of the fatty acid

1050 oxidation which triggers the expression β oxidation enzymes in the liver. FOXO is a metabolic

1051 regulatory transcription factor that down regulates glycolysis and influences on the

1052 gluconeogenic gene expression under fasting condition. TRB3 is another transcription factor

1053   i.e.activated by PPARα in response to the fatty acids and glucagon signaling which further

1054   inhibits AKT activation thereby down regulating the effect of insulin signaling. Furthermore, a

1055   major regulator of energy homeostasis is AMP activated protein kinase which is activated under

1056   energy stress or starvation, due to the changes in the AMP/ATP ratios in the cell. It is a potent

1057   transcriptional regulator that down regulates the anabolic pathways such as glycogen synthesis,

1058   fatty acid synthesis and protein synthesis.

1059 $\frac{dT_i}{dt} = T_{synth} + \left(\sum_{j=1}^{nj} T\_act_j * T_i\right) * T\_Areg_p * T\_Dreg_j - T_{deg} * \left(\sum_{k=1}^{nk} T\_dacts_k\right) * T_i (19)$

1060 $T\_Areg_p = \prod_p^{pn}\left(\frac{A_p{}^n}{A_p{}^n + K_p{}^n}\right)(20)$

1061 $T\_Dreg_j = \prod_q^{qn}\left(\frac{K_q{}^n}{I_p{}^n + K_p{}^n}\right)(21)$

1062   Where, T_{synth} and T_{deg} are the basal synthesis and degradation rate of ith transcription factor

1063   T,T_act_j and T_dact_k are the activation rates of the expression and degradation of the

1064   transcriptional factor, respectively. T_Areg_p and T_dpreg_p are the product of regulatory

1065   interactions of that actvate and deactivate the transcriptional factor T, respectively. A_p and I_p are

1066   the activator and inhibitor concentrations, respectively.

1067   **Table IV** Regulation of Transcriptional factors by signaling components and macronutrients.

Transcription Factors	Positive Regulation	Negative Regulation	References
SREBP	S6K, AKT, PKC	cAMP, FOXO, AMPK,	(119,127)
ChREBP	Glucose,	PKA, AMPK	(121,128)

PPARγ	AKT, FFA,	AMPK	(122,129)
PPARα	PKA, FFA, PGC		(130)
CREB	PKA,	AKT	(131,132)
CEBPa	cAMP	PKC,	(124,133)
TRB3	PI3K, PKC, PPAR, PGC1		(134,135)
PGC1	FOXO, CREB	AKT,	(136)
FOXO	Glnac, AMPK,	AKT, PPARγ	(137,125)
AMPK	AMP	AKT,PKA, ATP	(126)

1068

1069 **References**

1070 1. Chandramouli V, Ekberg K, Schumann WC, Kalhan SC, Wahren J, Landau BR. Quantifying
1071 gluconeogenesis during fasting. Am J Physiol - Endocrinol Metab. 1997;273(6 36-6):E1209–15.

1072 2. Radziuk J, Pye S. Hepatic glucose uptake, gluconeogenesis and the regulation of glycogen
1073 synthesis. Diabetes Metab Res Rev. 2001;17(4):250–72.

1074 3. Chen X, Iqbal N, Boden G. The effects of free fatty acids on gluconeogenesis and glycogenolysis in
1075 normal subjects. J Clin Invest. 1999;103(3):365–72.

1076 4. Pilkis SJ, Granner DK. Molecular physiology of the regulation of hepatic gluconeogenesis and
1077 glycolysis. Annu Rev Physiol. 1992;54:885–909.

1078 5. Kitano H, Oda K, Kimura T, Matsuoka Y, Csete M, Doyle J, et al. Metabolic syndrome and
1079 robustness tradeoffs. Diabetes. 2004;53(suppl 3):S6–15.

1080 6. Kudchodkar BJ, Lee MJ, Lee SM, DiMarco NM, Lacko AG. Effect of dietary protein on cholesterol
1081 homeostasis in diabetic rats. J Lipid Res. 1988;29(10):1272–87.

1082 7. Liao C-C, Lin Y-L, Kuo C-F. Effect of High-Fat Diet on Hepatic Proteomics of Hamsters. J Agric Food
1083 Chem. 2015 Feb 18;63(6):1869–81.

1084 8. Pichon L, Huneau J-F, Fromentin G, Tomé D. A high-protein, high-fat, carbohydrate-free diet
1085 reduces energy intake, hepatic lipogenesis, and adiposity in rats. J Nutr. 2006;136(5):1256–60.

1086 9. Podolin DA, Wei Y, Pagliassotti MJ. Effects of a high-fat diet and voluntary wheel running on
1087 gluconeogenesis and lipolysis in rats. J Appl Physiol. 1999;86(4):1374–80.

1088   10.   Satabin P, Bois-Joyeux B, Chanez M, Guezennec CY, Peret J. Effects of long-term feeding of high-
1089   protein or high-fat diets on the response to exercise in the rat. Eur J Appl Physiol.
1090   1989;58(6):583–90.

1091   11.   Satapati S, Sunny NE, Kucejova B, Fu X, He TT, Mendez-Lucas A, et al. Elevated TCA cycle function
1092   in the pathology of diet-induced hepatic insulin resistance and fatty liver. J Lipid Res. 2012 Jun
1093   1;53(6):1080–92.

1094   12.   Schindler, C, Felber JP. Study on the effect of a high fat diet on diaphragm and liver glycogen and
1095   glycerides in the rat. Horm Metab Res 1986 Feb18291-3. 1986 Feb;18(2)(91-3).

1096   13.   Schwarz J, Tomé D, Baars A, Hooiveld GJEJ, Müller M. Dietary Protein Affects Gene Expression
1097   and Prevents Lipid Accumulation in the Liver in Mice. Blanc S, editor. PLoS ONE. 2012 Oct
1098   23;7(10):e47303.

1099   14.   Sunny NE, Parks EJ, Browning JD, Burgess SC. Excessive Hepatic Mitochondrial TCA Cycle and
1100   Gluconeogenesis in Humans with Nonalcoholic Fatty Liver Disease. Cell Metab. 2011
1101   Dec;14(6):804–10.

1102   15.   Bechmann LP, Hannivoort R, Gerken G, Hotamisligi GS, Trauner M, Canbay A. The interaction of
1103   hepatic lipid and glucose metabolism in liver diseases. J Hepatol. 2012;56:952–64.

1104   16.   Chevalier S, Burgess SC, Malloy CR, Gougeon R, Marliss EB, Morais JA. The greater contribution of
1105   gluconeogenesis to glucose production in obesity is related to increased whole-body protein
1106   catabolism. Diabetes. 2006;55(3):675–81.

1107   17.   Perry RJ, Samuel VT, Petersen KF, Shulman GI. The role of hepatic lipids in hepatic insulin
1108   resistance and type 2 diabetes. Nature. 2014 Jun 4;510(7503):84–91.

1109   18.   Keane K, Newsholme P. Chapter One - Metabolic Regulation of Insulin Secretion. In: Gerald
1110   Litwack, editor. Vitamins & Hormones [Internet]. Academic Press; 2014. p. 1–33. Available from:
1111   http://www.sciencedirect.com/science/article/pii/B9780128001745000016

1112   19.   Newsholme P, Cruzat V, Arfuso F, Keane K. Nutrient regulation of insulin secretion and action. J
1113   Endocrinol. 2014 Jun 1;221(3):R105–20.

1114   20.   Newsholme P, Gaudel C, McClenaghan N. Nutrient Regulation of Insulin Secretion and β-Cell
1115   Functional Integrity. In: Islam MS, editor. The Islets of Langerhans [Internet]. Springer
1116   Netherlands; 2010. p. 91–114. Available from: http://dx.doi.org/10.1007/978-90-481-3271-3_6

1117   21.   Gual P, Le Marchand-Brustel Y, Tanti J-F. Positive and negative regulation of insulin signaling
1118   through IRS-1 phosphorylation. Biochimie. 2005 Jan;87(1):99–109.

1119   22.   Lansard M, Panserat S, Plagnes-Juan E, Seiliez I, Skiba-Cassy S. Integration of insulin and amino
1120   acid signals that regulate hepatic metabolism-related gene expression in rainbow trout: role of
1121   TOR. Amino Acids. 2010 Aug;39(3):801–10.

1122   23.   Weickert MO, Pfeiffer AFH. Signalling mechanisms linking hepatic glucose and lipid metabolism.
1123   Diabetologia. 2006 Aug;49(8):1732–41.

1124 24. Breda E, Cobelli C. Insulin Secretion Rate During Glucose Stimuli: Alternative Analyses of C-
1125 Peptide Data. Ann Biomed Eng. 2001 Aug;29(8):692–700.

1126 25. Sherwin RS, Kramer KJ, Tobin JD, Insel PA, Liljenquist JE, Berman M, et al. A model of the kinetics
1127 of insulin in man. J Clin Invest. 1974;53(5):1481.

1128 26. Toffolo G. A minimal model of insulin secretion and kinetics to assess hepatic insulin extraction.
1129 AJP Endocrinol Metab. 2005 Sep 20;290(1):E169–76.

1130 27. Mingrone G. Dietary fatty acids and insulin secretion. Scand J Food Nutr. 2006;50(1):79–84.

1131 28. Lam TKT, Yoshii H, Haber CA, Bogdanovic E, Lam L, Fantus IG, et al. Free fatty acid-induced
1132 hepatic insulin resistance: a potential role for protein kinase C-δ. Am J Physiol - Endocrinol
1133 Metab. 2002 Oct 1;283(4):E682–91.

1134 29. Pereira S, Park E, Mori Y, Haber CA, Han P, Uchida T, et al. FFA-induced Hepatic Insulin Resistance
1135 in vivo is mediated by PKC-δ, NADPH Oxidase, and Oxidative Stress. Am J Physiol - Endocrinol
1136 Metab [Internet]. 2014 May 13; Available from:
1137 http://ajpendo.physiology.org/content/early/2014/05/08/ajpendo.00436.2013.abstract

1138 30. Beard DA. Thermodynamic-based computational profiling of cellular regulatory control in
1139 hepatocyte metabolism. AJP Endocrinol Metab. 2004 Oct 26;288(3):E633–44.

1140 31. Blavy P, Gondret F, Guillou H, Lagarrigue S, Martin P, Radulescu O, et al. A minimal and dynamic
1141 model for fatty acid metabolism in mouse liver. In: Journées Ouvertes de Biologie, Informatique
1142 et Mathématique (JOBIM) [Internet]. 2008 [cited 2015 Jul 25]. Available from: https://hal-
1143 agrocampus-ouest.archives-ouvertes.fr/hal-00729742/

1144 32. Calvetti D, Kuceyeski A, Somersalo E. A mathematical model of liver metabolism: from steady
1145 state to dynamic. J Phys Conf Ser. 2008 Jul 1;124:012012.

1146 33. Chalhoub E, Hanson RW, Belovich JM. A computer model of gluconeogenesis and lipid
1147 metabolism in the perfused liver. AJP Endocrinol Metab. 2007 Oct 23;293(6):E1676–86.

1148 34. De Maria C, Grassini D, Vozzi F, Vinci B, Landi A, Ahluwalia A, et al. HEMET: Mathematical model
1149 of biochemical pathways for simulation and prediction of HEpatocyte METabolism. Comput
1150 Methods Programs Biomed. 2008 Oct;92(1):121–34.

1151 35. Dean JT, Rizk ML, Tan Y, Dipple KM, Liao JC. Ensemble Modeling of Hepatic Fatty Acid Metabolism
1152 with a Synthetic Glyoxylate Shunt. Biophys J. 2010 Apr;98(8):1385–95.

1153 36. Gille C, Bölling C, Hoppe A, Bulik S, Hoffmann S, Hübner K, et al. HepatoNet1: a comprehensive
1154 metabolic reconstruction of the human hepatocyte for the analysis of liver physiology. Mol Syst
1155 Biol [Internet]. 2010 Sep 7 [cited 2014 Apr 30];6. Available from:
1156 http://msb.embopress.org/cgi/doi/10.1038/msb.2010.62

1157 37. Hetherington J, Sumner T, Seymour RM, Li L, Rey MV, Yamaji S, et al. A composite computational
1158 model of liver glucose homeostasis. I. Building the composite model. J R Soc Interface. 2012 Apr
1159 7;9(69):689–700.

1160   38.   König M, Bulik S, Holzhütter H-G. Quantifying the Contribution of the Liver to Glucose
1161   Homeostasis: A Detailed Kinetic Model of Human Hepatic Glucose Metabolism. Papin JA, editor.
1162   PLoS Comput Biol. 2012 Jun 21;8(6):e1002577.

1163   39.   Orman MA, Mattick J, Androulakis IP, Berthiaume F, Ierapetritou MG. Stoichiometry Based
1164   Steady-State Hepatic Flux Analysis: Computational and Experimental Aspects. Metabolites. 2012
1165   Mar 14;2(4):268–91.

1166   40.   Rausova Z, Chrenova J, Nuutila P, Iozzo P, Dedik L. System approach to modeling of liver glucose
1167   metabolism with physiologically interpreted model parameters outgoing from [18F]FDG
1168   concentrations measured by PET. Comput Methods Programs Biomed. 2012 Aug;107(2):347–56.

1169   41.   Shorten PR, Upreti GC. A mathematical model of fatty acid metabolism and VLDL assembly in
1170   human liver. Biochim Biophys Acta BBA - Mol Cell Biol Lipids. 2005 Sep;1736(2):94–108.

1171   42.   Xu K, Morgan KT, Todd Gehris A, Elston TC, Gomez SM. A Whole-Body Model for Glycogen
1172   Regulation Reveals a Critical Role for Substrate Cycling in Maintaining Blood Glucose
1173   Homeostasis. Price ND, editor. PLoS Comput Biol. 2011 Dec 1;7(12):e1002272.

1174   43.   Sedaghat AR, Sherman A, Quon MJ. A mathematical model of metabolic insulin signaling
1175   pathways. Am J Physiol - Endocrinol Metab. 2002 Nov 1;283(5):E1084–101.

1176   44.   Mutalik VK, Venkatesh KV. Quantification of the glycogen cascade system: the ultrasensitive
1177   responses of liver glycogen synthase and muscle phosphorylase are due to distinctive regulatory
1178   designs. Theor Biol Med Model. 2005;2(1):19.

1179   45.   Vinod PKU, Venkatesh KV. Quantification of the effect of amino acids on an integrated mTOR and
1180   insulin signaling pathway. Mol Biosyst. 2009;5(10):1163.

1181   46.   Dalla Man C, Rizza RA, Cobelli C. Meal Simulation Model of the Glucose-Insulin System. IEEE Trans
1182   Biomed Eng. 2007 Oct;54(10):1740–9.

1183   47.   Wang L, Yu J, Walzem RL. High-carbohydrate diets affect the size and composition of plasma
1184   lipoproteins in hamsters (Mesocricetus auratus). Comp Med. 2008;58(2):151.

1185   48.   Belfiore F, Iannello S. A formula for quantifying the effects of substrate cycles (futile cycles) on
1186   metabolic regulation. Its application to glucose futile cycle in liver as studied by glucose-6-
1187   phosphatase/glucokinase determinations. Acta Diabetol Lat. 1990;27(1):71–80.

1188   49.   Jump DB, Botolin D, Wang Y, Xu J, Christian B, Demeure O. Fatty acid regulation of hepatic gene
1189   transcription. J Nutr. 2005;135(11):2503–6.

1190   50.   Rafoth RJ, Onstad GR. Urea synthesis after oral protein ingestion in man. J Clin Invest.
1191   1975;56(5):1170.

1192   51.   van de Poll MCG, Wigmore SJ, Redhead DN, Beets-Tan RGH, Garden OJ, Greve JWM, et al. Effect
1193   of major liver resection on hepatic ureagenesis in humans. AJP Gastrointest Liver Physiol. 2007
1194   Sep 27;293(5):G956–62.

1195 52. Nuttall FQ, Ngo A, Gannon MC. Regulation of hepatic glucose production and the role of
1196   gluconeogenesis in humans: Is the rate of gluconeogenesis constant? Diabetes Metab Res Rev.
1197   2008;24(6):438–58.

1198 53. Fromenti C, Azzout-Marniche D, Stepien M, Even P, Fromentin G, Tomé D, et al. Whole body
1199   amino acids are candidate precursors of postprandial hepatic neoglycogenogenesis in high
1200   protein fed rats. FASEB J. 2009 Apr;23(738.9).

1201 54. Veldhorst MA, Westerterp-Plantenga MS, Westerterp KR. Gluconeogenesis and energy
1202   expenditure after a high-protein, carbohydrate-free diet. Am J Clin Nutr. 2009 Sep 1;90(3):519–
1203   26.

1204 55. Krssak M, Brehm A, Bernroider E, Anderwald C, Nowotny P, Dalla Man C, et al. Alterations in
1205   postprandial hepatic glycogen metabolism in type 2 diabetes. Diabetes. 2004;53(12):3048–56.

1206 56. Roden M. Clinical Diabetes Research: Methods and Techniques. John Wiley and Sons; 2007.

1207 57. Ulusoy E, Eren B. Histological changes of liver glycogen storage in mice (Mus musculus) caused by
1208   high-protein diets. 2006 [cited 2015 Jul 25]; Available from:
1209   https://digitum.um.es/xmlui/handle/10201/22701

1210 58. Taylor R, Magnusson I, Rothman DL, Cline GW, Caumo A, Cobelli C, et al. Direct assessment of
1211   liver glycogen storage by 13C nuclear magnetic resonance spectroscopy and regulation of glucose
1212   homeostasis after a mixed meal in normal subjects. J Clin Invest. 1996;97(1):126.

1213 59. Krízová E, Simek V. Effect of intermittent feeding with high-fat diet on changes of glycogen,
1214   protein and fat content in liver and skeletal muscle in the laboratory mouse. Physiol Res.
1215   1996;45((5)):379–83.

1216 60. Owen OE, Kalhan SC, Hanson RW. The Key Role of Anaplerosis and Cataplerosis for Citric Acid
1217   Cycle Function. J Biol Chem. 2002 Aug 23;277(34):30409–12.

1218 61. Ferramosca A, Conte A, Damiano F, Siculella L, Zara V. Differential effects of high-carbohydrate
1219   and high-fat diets on hepatic lipogenesis in rats. Eur J Nutr. 2014 Jun;53(4):1103–14.

1220 62. Petzke K, Freudenberg A, Klaus S. Beyond the Role of Dietary Protein and Amino Acids in the
1221   Prevention of Diet-Induced Obesity. Int J Mol Sci. 2014 Jan 20;15(1):1374–91.

1222 63. Nakano K, Ashida K. Effect of Dietary Carbohydrate and Fat on Amino Acid-degrading
1223   Enzymes in Relation to Their Protein Sparing Action. J Nutr. 1969;100:208–2016.

1224 64. Garcia-Caraballo SC, Comhair TM, Verheyen F, Gaemers I, Schaap FG, Houten SM, et al.
1225   Prevention and reversal of hepatic steatosis with a high-protein diet in mice. Biochim Biophys
1226   Acta BBA - Mol Basis Dis. 2013 May;1832(5):685–95.

1227 65. Cahova M, Dankova H, Palenickova E, Papackova Z, Kazdova L. The Opposite Effects of High-
1228   Sucrose and High-Fat Diet on Fatty Acid Oxidation and Very Low Density Lipoprotein Secretion in
1229   Rat Model of Metabolic Syndrome. J Nutr Metab. 2012;2012:1–10.

1230 66. Silbernagel G, Lütjohann D, Machann J, Meichsner S, Kantartzis K, Schick F, et al. Cholesterol
1231 Synthesis Is Associated with Hepatic Lipid Content and Dependent on Fructose/Glucose Intake in
1232 Healthy Humans. Exp Diabetes Res. 2012;2012:1–7.

1233 67. Raymond F, Wang L, Moser M, Metairon S, Mansourian R, Zwahlen M-C, et al. Consequences of
1234 Exchanging Carbohydrates for Proteins in the Cholesterol Metabolism of Mice Fed a High-fat Diet.
1235 Blanc S, editor. PLoS ONE. 2012 Nov 6;7(11):e49058.

1236 68. Clarke SD, Romsos DR, Tsai AC, Belo PS, LEVEILLE WBAA. Studies oÃ-the Effect of Dietary
1237 Cholesterol on Hepatic Protein Synthesis, Reduced Glutathione Levels and Serine Dehydratase
1238 Activity in the Rat1. J Nutr. 1976;106:94–102.

1239 69. Rafoth RJ, Onstad GR. Urea synthesis after oral protein ingestion in man. J Clin Invest.
1240 1975;56(5):1170.

1241 70. Wiechetek M, Breves G, Höller H. Effects of increased blood ammonia concentrations on the
1242 concentrations of some metabolites in rat tissues. Q J Exp Physiol. 1981;66(4):423–9.

1243 71. Cherrington AD, Lecture B. Control of glucose uptake and release by the liver in vivo. DIABETES-N
1244 Y-. 1999;48:1198–214.

1245 72. Girard J. The Inhibitory Effects of Insulin on Hepatic Glucose Production Are Both Direct and
1246 Indirect. Diabetes. 2006 Dec 1;55(Supplement 2):S65–9.

1247 73. Baum JI, Layman DK, Freund GG, Rahn KA, Nakamura MT, Yudell BE. A reduced carbohydrate,
1248 increased protein diet stabilizes glycemic control and minimizes adipose tissue glucose disposal in
1249 rats. J Nutr. 2006;136(7):1855–61.

1250 74. Brøns C, Jensen CB, Storgaard H, Hiscock NJ, White A, Appel JS, et al. Impact of short-term high-
1251 fat feeding on glucose and insulin metabolism in young healthy men: High-fat feeding in young
1252 healthy men. J Physiol. 2009 May 15;587(10):2387–97.

1253 75. Bisschop PH, de Metz J, Ackermans MT, Endert E, Pijl H, Kuipers F, et al. Dietary fat content alters
1254 insulin-mediated glucose metabolism in healthy men. Am J Clin Nutr. 2001;73(3):554–9.

1255 76. Henkel E, Menschikowski M, Koehler C, Leonhardt W, Hanefeld M. Impact of glucagon response
1256 on postprandial hyperglycemia in men with impaired glucose tolerance and type 2 diabetes
1257 mellitus. Metabolism. 2005;54(9):1168–73.

1258 77. de Meijer VE, Le HD, Meisel JA, Sharif MRA, Pan A, Nosé V, et al. Dietary fat intake promotes the
1259 development of hepatic steatosis independently from excess caloric consumption in a murine
1260 model. Metabolism. 2010 Aug;59(8):1092–105.

1261 78. Nguyen P, Leray V, Diez M, Serisier S, Bloc'h JL, Siliart B, et al. Liver lipid metabolism. J Anim
1262 Physiol Anim Nutr. 2008 Jun;92(3):272–83.

1263 79. Mashek DG. Hepatic Fatty Acid Trafficking: Multiple Forks in the Road. Adv Nutr Int Rev J. 2013
1264 Nov 1;4(6):697–710.

1265 80. Leavens KF, Birnbaum MJ. Insulin signaling to hepatic lipid metabolism in health and disease. Crit
1266 Rev Biochem Mol Biol. 2011 Jun;46(3):200–15.

1267　81.　Samuel VT, Petersen KF, Shulman GI. Lipid-induced insulin resistance: unravelling the mechanism.
1268　　　　The Lancet. 2010;375(9733):2267–77.

1269　82.　Jornayvaz FR, Shulman GI. Diacylglycerol Activation of Protein Kinase Cε and Hepatic Insulin
1270　　　　Resistance. Cell Metab. 2012 May;15(5):574–84.

1271　83.　Birkenfeld AL, Shulman GI. Nonalcoholic fatty liver disease, hepatic insulin resistance, and type 2
1272　　　　diabetes. Hepatology. 2014;59(2):713–23.

1273　84.　Chalhoub E, Xie L, Balasubramanian V, Kim J, Belovich J. A distributed model of carbohydrate
1274　　　　transport and metabolism in the liver during rest and high-intensity exercise. Ann Biomed Eng.
1275　　　　2007;35(3):474–91.

1276　85.　Somvanshi PR, Venkatesh KV. A conceptual review on systems biology in health and diseases:
1277　　　　from biological networks to modern therapeutics. Syst Synth Biol. 2014 Mar;8(1):99–116.

1278　86.　Calbet JA, MacLean DA. Plasma glucagon and insulin responses depend on the rate of appearance
1279　　　　of amino acids after ingestion of different protein solutions in humans. J Nutr. 2002;132(8):2174–
1280　　　　82.

1281　87.　Floyd JC, Fajans SS, Pek S, Thiffault CA, Knopf RF, Conn JW. Synergistic effect of essential amino
1282　　　　acids and glucose upon insulin secretion in man. Diabetes. 1970;19(2):109–15.

1283　88.　van Loon LJ, Saris WH, Verhagen H, Wagenmakers AJ. Plasma insulin responses after ingestion of
1284　　　　different amino acid or protein mixtures with carbohydrate. Am J Clin Nutr. 2000;72(1):96–105.

1285　89.　Nyman E, Brannmark C, Palmer R, Brugard J, Nystrom FH, Stralfors P, et al. A Hierarchical Whole-
1286　　　　body Modeling Approach Elucidates the Link between in Vitro Insulin Signaling and in Vivo
1287　　　　Glucose Homeostasis. J Biol Chem. 2011 Jul 22;286(29):26028–41.

1288　90.　Dash RK, Yanjun Li, Jaeyeon Kim, Saidel GM, Cabrera ME. Modeling Cellular Metabolism and
1289　　　　Energetics in Skeletal Muscle: Large-Scale Parameter Estimation and Sensitivity Analysis. IEEE
1290　　　　Trans Biomed Eng. 2008 Apr;55(4):1298–318.

1291　91.　Keane K, Newsholme P. Chapter One - Metabolic Regulation of Insulin Secretion. In: Gerald
1292　　　　Litwack, editor. Vitamins & Hormones [Internet]. Academic Press; 2014. p. 1–33. Available from:
1293　　　　http://www.sciencedirect.com/science/article/pii/B9780128001745000016

1294　92.　Matveyenko AV, Liuwantara D, Gurlo T, Kirakossian D, Dalla Man C, Cobelli C, et al. Pulsatile
1295　　　　Portal Vein Insulin Delivery Enhances Hepatic Insulin Action and Signaling. Diabetes. 2012 Sep
1296　　　　1;61(9):2269–79.

1297　93.　Gravena C, Mathias P, Ashcroft S. Acute effects of fatty acids on insulin secretion from rat and
1298　　　　human islets of Langerhans. J Endocrinol. 2002 Apr 1;173(1):73–80.

1299　94.　Manco M, Calvani M, Mingrone G. Effects of dietary fatty acids on insulin sensitivity and
1300　　　　secretion. Diabetes, Obesity and Metabolism. Diabetes Obes Metab. 6:402–13.

1301　95.　González-Vélez V, Dupont G, Gil A, González A, Quesada I. Model for Glucagon Secretion by
1302　　　　Pancreatic α-Cells. Maedler K, editor. PLoS ONE. 2012 Mar 7;7(3):e32282.

1303   96.   Ainscow EK, Brand MD. The responses of rat hepatocytes to glucagon and adrenaline. Eur J
1304   Biochem. 1999;265(3):1043–55.

1305   97.   Pagliara AS, Stillings SN, Haymond MW, Hover BA, Matschinsky FM. Insulin and glucose as
1306   modulators of the amino acid-induced glucagon release in the isolated pancreas of alloxan and
1307   streptozotocin diabetic rats. J Clin Invest. 1975;55(2):244.

1308   98.   Henningsson R, Lundquist I. Arginine-induced insulin release is decreased and glucagon increased
1309   in parallel with islet NO production. Am J Physiol-Endocrinol Metab. 1998;275(3):E500–6.

1310   99.   Frayn KN. Metabolic Regulation: A Human Perspective. 2010.

1311   100. Watterson S, Guerriero ML, Blanc M, Mazein A, Loewe L, Robertson KA, et al. A model of flux
1312   regulation in the cholesterol biosynthesis pathway: Immune mediated graduated flux reduction
1313   versus statin-like led stepped flux reduction. Biochimie. 2013 Mar;95(3):613–21.

1314   101. Hanover JA, Krause MW, Love DC. The hexosamine signaling pathway: O-GlcNAc cycling in feast
1315   or famine. Biochim Biophys Acta BBA - Gen Subj. 2010 Feb;1800(2):80–95.

1316   102. Iadicicco C. Mechanisms linking glucotoxicity to the development of insulin resistance: a role for
1317   the endoplasmic reticulum stress [Internet]. Università degli studi di Napoli Federico II; 2010
1318   [cited 2014 Apr 29]. Available from: http://www.fedoa.unina.it/7982/

1319   103. Halperin ML, Robinson BH, Fritz IB. Effects of palmitoyl CoA on citrate and malate transport by rat
1320   liver mitochondria. Proc Natl Acad Sci. 1972;69(4):1003–7.

1321   104. Inoki K, Li Y, Zhu T, Wu J, Guan K-L. TSC2 is phosphorylated and inhibited by Akt and suppresses
1322   mTOR signalling. Nat Cell Biol. 2002 Sep;4(9):648–57.

1323   105. Laplante M, Sabatini DM. mTOR Signaling in Growth Control and Disease. Cell. 149(2):274–93.

1324   106. Li S, Brown MS, Goldstein JL. Bifurcation of insulin signaling pathway in rat liver: mTORC1
1325   required for stimulation of lipogenesis, but not inhibition of gluconeogenesis. Proc Natl Acad Sci.
1326   2010 Feb 23;107(8):3441–6.

1327   107. Dalle Pezze P, Sonntag AG, Thien A, Prentzell MT, Godel M, Fischer S, et al. A dynamic network
1328   model of mTOR signaling reveals TSC-independent mTORC2 regulation. Sci Signal.
1329   2012;5(217):ra25.

1330   108. Sumner T. Sensitivity analysis in Systems biology modelling And its application to a Multi-scale
1331   model of blood Glucose homeostasis. Univ. College London;

1332   109. Wullschleger S, Loewith R, Hall MN. TOR Signaling in Growth and Metabolism. Cell. 2006
1333   Feb;124(3):471–84.

1334   110. Tremblay F, Marette A. Amino acid and insulin signaling via the mTOR/p70 S6 kinase pathway A
1335   negative feedback mechanism leading to insulin resistance in skeletal muscle cells. J Biol Chem.
1336   2001;276(41):38052–60.

1337   111. Shaw RJ. LKB1 and AMP-activated protein kinase control of mTOR signalling and growth. Acta
1338   Physiol. 2009;196(1):65–80.

1339 112. Manning BD, Logsdon MN, Lipovsky AI, Abbott D, Kwiatkowski DJ, Cantley LC. Feedback inhibition
1340   of Akt signaling limits the growth of tumors lacking Tsc2. Genes Dev. 2005 Aug 1;19(15):1773–8.

1341 113. Hanson MS, Stephenson AH, Bowles EA, Sprague RS. Insulin inhibits human erythrocyte cAMP
1342   accumulation and ATP release: role of phosphodiesterase 3 and phosphoinositide 3-kinase. Exp
1343   Biol Med. 2010 Feb 1;235(2):256–62.

1344 114. Rendell M, Salomon Y, Lin MC, Rodbell M, Berman M. The hepatic adenylate cyclase system. III. A
1345   mathematical model for the steady state kinetics of catalysis and nucleotide regulation. J Biol
1346   Chem. 1975;250(11):4253–60.

1347 115. Ni Q, Ganesan A, Aye-Han N-N, Gao X, Allen MD, Levchenko A, et al. Signaling diversity of PKA
1348   achieved via a Ca2+-cAMP-PKA oscillatory circuit. Nat Chem Biol. 2011 Jan;7(1):34–40.

1349 116. Omori K, Kotera J. Overview of PDEs and Their Regulation. Circ Res. 2007 Feb 16;100(3):309–27.

1350 117. Desvergne B. Transcriptional Regulation of Metabolism. Physiol Rev. 2006 Apr 1;86(2):465–514.

1351 118. Nadeau KJ. Insulin Regulation of Sterol Regulatory Element-binding Protein-1 Expression in L-6
1352   Muscle Cells and 3T3 L1 Adipocytes. J Biol Chem. 2004 Jun 23;279(33):34380–7.

1353 119. Feleischmann M, Iynedjian P. Regulation of sterol regulatory-element binding protein 1 gene
1354   expression in liver: role of insulin and protein kinase B/cAkt. Biochem J. 2000;349:13–7.

1355 120. Foretz M, Guichard C, Ferré P, Foufelle F. Sterol regulatory element binding protein-1c is a major
1356   mediator of insulin action on the hepatic expression of glucokinase and lipogenesis-related
1357   genes. Proc Natl Acad Sci. 1999;96(22):12737–42.

1358 121. Iizuka K, Bruick RK, Liang G, Horton JD, Uyeda K. Deficiency of carbohydrate response element-
1359   binding protein (ChREBP) reduces lipogenesis as well as glycolysis. Proc Natl Acad Sci U S A.
1360   2004;101(19):7281–6.

1361 122. König B, Koch A, Spielmann J, Hilgenfeld C, Hirche F, Stangl GI, et al. Activation of PPARα and
1362   PPARγ reduces triacylglycerol synthesis in rat hepatoma cells by reduction of nuclear SREBP-1.
1363   Eur J Pharmacol. 2009 Mar;605(1-3):23–30.

1364 123. Rakhshandehroo M, Sanderson LM, Matilainen M, Stienstra R, Carlberg C, de Groot PJ, et al.
1365   Comprehensive Analysis of PPARα-Dependent Regulation of Hepatic Lipid Metabolism by
1366   Expression Profiling. PPAR Res. 2007;2007:1–13.

1367 124. Roesler WJ. The role of C/EBP in nutrient and hormonal regulation of gene expression. Annu Rev
1368   Nutr. 2001;21(1):141–65.

1369 125. Gross DN, van den Heuvel APJ, Birnbaum MJ. The role of FoxO in the regulation of metabolism.
1370   Oncogene. 2008 Apr 7;27(16):2320–36.

1371 126. Carling D. The AMP-activated protein kinase cascade – a unifying system for energy control.
1372   Trends Biochem Sci. 2004 Jan;29(1):18–24.

1373   127.   Owen JL, Zhang Y, Bae S-H, Farooqi MS, Liang G, Hammer RE, et al. Insulin stimulation of SREBP-
1374   1c processing in transgenic rat hepatocytes requires p70 S6-kinase. Proc Natl Acad Sci. 2012 Oct
1375   2;109(40):16184–9.

1376   128.   Benhamed F, Denechaud P-D, Lemoine M, Robichon C, Moldes M, Bertrand-Michel J, et al. The
1377   lipogenic transcription factor ChREBP dissociates hepatic steatosis from insulin resistance in mice
1378   and humans. J Clin Invest. 2012 Jun 1;122(6):2176–94.

1379   129.   Morán-Salvador E, López-Parra M, García-Alonso V, Titos E, Martínez-Clemente M, González-Périz
1380   A, et al. Role for PPARγ in obesity-induced hepatic steatosis as determined by hepatocyte- and
1381   macrophage-specific conditional knockouts. FASEB J. 2011 Aug 1;25(8):2538–50.

1382   130.   McMullen PD, Bhattacharya S, Woods CG, Sun B, Yarborough K, Ross SM, et al. A map of the
1383   PPARα transcription regulatory network for primary human hepatocytes. Chem Biol Interact.
1384   2014;209(1):14–24.

1385   131.   Everett L, Lay J, Lukovac S, Bernstein D, Steger D, Lazar M, et al. Integrative genomic analysis of
1386   CREB defines a critical role for transcription factor networks in mediating the fed/fasted switch in
1387   liver. BMC Genomics. 2013;14(1):337.

1388   132.   Herzig S, Long F, Jhala US, Hedrick S, Quinn R, Bauer A, et al. CREB regulates hepatic
1389   gluconeogenesis through the coactivator PGC-1. Nature. 2001 Sep 13;413(6852):179–83.

1390   133.   Wang N, Finegold M, Bradley A, Ou C, Abdelsayed S, Wilde M, et al. Impaired energy homeostasis
1391   in C/EBP alpha knockout mice. Science. 1995 Aug 25;269(5227):1108–12.

1392   134.   Rie Matsushima, NHN. Effect of TRB3 on Insulin and Nutrient-stimulated Hepatic p70 S6 Kinase
1393   Activity. J Biol Chem. 2006;281:29719–29.

1394   135.   Keyong Du, KD. TRB3-A tribble Homolog That Inhibits Akt/PKB Activation by Insulin in Liver.
1395   Science. 2003;300(1574).

1396   136.   Koo S-H, Satoh H, Herzig S, Lee C-H, Hedrick S, Kulkarni R, et al. PGC-1 promotes insulin resistance
1397   in liver through PPAR-α-dependent induction of TRB-3. Nat Med. 2004 May;10(5):530–4.

1398   137.   Hay N. Interplay between FOXO, TOR, and Akt. Biochim Biophys Acta BBA - Mol Cell Res. 2011
1399   Nov;1813(11):1965–70.

1400

Graphical Abstract

The hepatic metabolic functions are mediated by several pathways which are regulated at metabolic, signaling and transcriptional levels. These multilevel regulations with crosstalk between pathways constitutes a complex network which orchestrate together to provide a robust metabolic regulation in liver. The model analysis highlights the effect of plasma macronutrients namely, glucose, amino acids and fatty acids on these regulatory mechanisms to facilitate homeostasis. The insights were further used to explain experimental observations of several investigations reported in literature, through the regulatory mechanisms. Our analysis indicates that higher levels (above 2.5-3 fold) of macronutrients in plasma result in insulin resistance through disturbances at multiple levels i.e. metabolic, signaling and transcription.